

# Infinite efficiency of collisional Penrose process: Can over-spinning Kerr geometry be the source of ultra-high-energy cosmic rays and neutrinos ?

<sup>1</sup>Mandar Patil\*, <sup>1</sup>Tomohiro Harada<sup>†</sup>,

<sup>2</sup>Ken-ichi Nakao<sup>‡</sup>, <sup>3</sup>Pankaj S. Joshi<sup>§</sup>, <sup>4,5</sup>Masashi Kimura<sup>¶</sup>

<sup>1</sup>*Department of Physics, Rikkyo University, Toshima-ku, Tokyo 171-8501 Japan.*

<sup>2</sup>*Department of Mathematics and Physics, Graduate School of Science,  
Osaka City University, Osaka 558-8585, Japan.*

<sup>3</sup>*Tata Institute of Fundamental Research,  
Homi Bhabha Road, Mumbai 400005, India.*

<sup>4</sup>*DAMTP, Centre for Mathematical Sciences, University of Cambridge,  
Wilberforce Road, Cambridge CB3 0WA, United Kingdom.*

<sup>5</sup>*CENTRA, Departamento de Física, Instituto Superior Técnico-IST,  
Universidade de Lisboa-UL, Avenida Rovisco Pais 1, 1049 Lisboa, Portugal*

PACS numbers: 04.20.Dw, 04.70.-s, 04.70.Bw

---

\* Electronic address: mandar@rikkyo.ac.jp, mandarppatil@gmail.com

† Electronic address: harada@rikkyo.ac.jp

‡ Electronic address: knakao@sci.osaka-cu.ac.jp

§ Electronic address: psj@tifr.res.in

¶ Electronic address: masashi.kimura@tecnico.ulisboa.pt

## Abstract

The origin of the ultra-high-energy particles we receive on the Earth from the outer space such as EeV cosmic rays and PeV neutrinos remains an enigma. All mechanisms known to us currently make use of electromagnetic interaction to accelerate charged particles. In this paper we propose a mechanism exclusively based on gravity rather than electromagnetic interaction. We show that it is possible to generate ultra-high-energy particles starting from particles with moderate energies using the collisional Penrose process in an overspinning Kerr spacetime transcending the Kerr bound only by an infinitesimal amount, i.e., with the Kerr parameter  $a = M(1 + \epsilon)$ , where we take the limit  $\epsilon \rightarrow 0^+$ . We consider two massive particles starting from rest at infinity that collide at  $r = M$  with divergent center-of-mass energy and produce two massless particles. We show that massless particles produced in the collision can escape to infinity with the ultra-high energies exploiting the collisional Penrose process with the divergent efficiency  $\eta \sim 1/\sqrt{\epsilon} \rightarrow \infty$ . Assuming the isotropic emission of massless particles in the center-of-mass frame of the colliding particles, we show that half of the particles created in the collisions escape to infinity with the divergent energies, while the proportion of particles that reach infinity with finite energy is minuscule. To a distant observer, ultra-high-energy particles appear to originate from a bright spot which is at the angular location  $\xi \sim 2M/r_{obs}$  with respect to the singularity on the side which is rotating towards the observer. We compute the spectrum of the high energy massless particles and show that anisotropy in the emission in the center-of-mass frame leaves a distinct signature on its shape. Since the anisotropy is dictated by the differential cross section of the underlying particle physics process, the observation of the spectrum can constrain the particle physics model and serve as a unique probe into fundamental physics at ultra-high energies at which particles collide. Thus, the existence of the near-extremal overspinning Kerr geometry in the Universe, either as a transient or permanent configuration, would have deep implications on astrophysics as well as fundamental particle physics.

## I. INTRODUCTION

The Earth is bombarded with cosmic rays from the outer space consisting of protons as well as nuclei such as iron with energies that extend all the way upto several hundreds of EeV [1],[2]. There is no general consensus as of now on the acceleration mechanism that is responsible for the generation of the EeV particles. Two leading mechanisms are 1. diffusive acceleration by shock waves, i.e., Fermi acceleration and 2. acceleration by electric fields generated by time varying magnetic fields, i.e., unipolar inductors (see [3],[4],[5] and references therein). The conditions conducive to the particle acceleration can be found in a wide variety of astrophysical settings such as neutron stars, gamma ray bursts, active galactic nuclei, colliding galaxies and so on. We note that all the proposed acceleration mechanisms make use of electromagnetic interaction to accelerate charged particles. Cosmic rays with energies beyond 60 EeV are expected to produce neutrinos as they interact with the cosmic microwave background photons [6],[7]. Neutrinos with the energies in the range 100 TeV to PeV have been observed recently [8],[9]. However the connection between the production of ultra-high-energy neutrinos and cosmic rays is far from being understood [10].

The origin of the ultra-high-energy particles continues to be an enigma and a topic of an active ongoing investigation. Hence it is worthwhile to look for the other mechanisms that could accelerate particles to high energies. In this paper we present a novel mechanism to generate high-energy particles that exclusively makes use of gravity rather than electromagnetic interaction.

The Kerr metric is one of the simplest and most elegant solution to the Einstein equations in general relativity which exhibits many remarkable features [11]. The Kerr solution represents a rotating black hole if the spin parameter is smaller than the mass, i.e.,  $a \leq M$ . For large enough values of the spin parameter, i.e.,  $a > M$ , the Kerr metric represents a rotating naked singularity. One of the interesting features associated with the Kerr solution is the dragging of inertial frames, as a consequence of which spacetime can host the particle orbits with negative energies in the region called ergosphere. It was argued by Penrose that if a particle disintegrates into two particles, wherein one of the particles is launched onto the orbit with negative energy, the other particle can have energy larger than that of the initial particle. This process is known as Penrose process [12],[13]. Thus, one can throw in a particle into the ergosphere from the distant location and get out a particle with larger energy. An analogous process was considered wherein two particles collide and scatter. One of the scattered particles moves along the negative energy orbit, whereas the other particle is now endowed with energy larger than the combined energy of the two colliding particles. This process is known as the collisional Penrose process. It was argued

that the efficiency of the Penrose process and collisional Penrose process, defined as the ratio of the energy output to the energy input admits an upper bound which is around 1.2 for Kerr black hole [14],[15],[16],[17].

Interest in the collisional Penrose process was revived recently in light of the re-discovery of the process of ultra-high-energy particle collision around the extremal Kerr black holes [18],[17],[19]. When a particle with a specific critical value of the angular momentum, which asymptotically approaches the event horizon of the extremal Kerr black hole, collides at the location close to event horizon, with another particle with a sub-critical angular momentum that is radially ingoing at the horizon, the center-of-mass energy of collision shows divergence. This is relevant from the point of view of particle physics processes such as dark matter annihilation for which the cross section is dismal at low energies and is expected to show an upward trend at high energies or the resonances which occur at high energies [20],[21]. Debris from the ultra-high-energy collisions around the extremal Kerr black hole escaping to infinity is expected to have imprinted on it the signature of the physics at high energies. It was shown that the energies of the particles which are generated in the ultra-high-energy collisions around the Kerr black hole that manage to escape to infinity would be finite despite the boost by the collisional Penrose process [22],[23]. The efficiency of the collisional Penrose process can go upto 1.4. The escape fraction, i.e., the fraction of the particles produced in the ultra-high-energy collision that escape to infinity was shown to be vanishingly small [24],[25],[26]. Thus, the significance of the process of ultra-high-energy collisions around Kerr black holes from an observational point of view is not very clear.

Recently, it was shown that the efficiency of the collisional Penrose process can be boosted up by one order of magnitude by considering a collision between the particle with angular momentum slightly larger than the critical value, which turns back as an outgoing particle with the vanishingly small outward velocity just outside the horizon due to the angular momentum barrier and a sub-critical ingoing particle. The critical particle was taken to be an ingoing particle at the collision in the earlier investigations. The upper bound on the efficiency was revised to be around 14 [27].

The collision between an outgoing sub-critical particle and ingoing sub-critical particle just outside the horizon of the extremal Kerr black hole was considered in [28]. The efficiency of the collisional Penrose process was shown to diverge in this case. However, the outgoing sub-critical particle must be produced in yet another collision just outside the horizon, since such a particle cannot start from the distant location and then turn back as an outgoing particle just outside the horizon and also it cannot emerge from the black hole as nothing comes out of the black hole. It was shown that it would be possible to produce an outgoing sub-critical particle in the

preceding collision only if one of the colliding particles is super-heavy with divergent mass. Thus, the overall efficiency in the process of multiple collisions turns out to be finite and can take values upto 14. We, however note that the efficiency of the collisional Penrose process in the extremal Reissner-Nordström black hole spacetime case can be arbitrarily large[29],[30],[31].

Thus, it is very unlikely that it would be possible to extract a large amount of energy from the Kerr black hole. In this paper, we go beyond the extremality and consider the over-spinning Kerr geometry. The spacetime does not admit an event horizon but has a singularity at  $r = 0$  in the equatorial plane, which is visible to a distant observer. There is a possibility that an overspinning Kerr geometry could arise as a transient configuration in the region exterior to the regular matter cloud that undergoes a gravitational collapse followed by a bounce, thereby avoiding the occurrence of the singularity [32]. It might also be possible to overspin a near-extremal Kerr black hole with a test particle [33]. However the self-force could act as a cosmic censor in this process [34],[35]. Recently it was argued that there are a number of ways by which the overspinning spacetime geometries can arise in the context of string theory which provides resolution of naked singularities [36]. For instance,  $5 + 1$  dimensional solutions to the heterotic string theory presented in [37], when looked at from the large distance, appear to be  $3 + 1$  dimensional spacetimes sourced by the overspinning naked singularities. When the singularity is approached, the two compactified extra spatial dimensions manifest themselves and the  $3 + 1$  dimensional singularity is resolved. The over-spinning naked singular geometry has been shown to be unstable to the linear perturbations [38],[39]. Their analysis assumes the spacetime to be  $3 + 1$  dimensional and that the overspinning Kerr geometry extends either throughout the spacetime or is valid outside the hyper-spinning object with the ingoing or reflecting boundary conditions imposed on its surface. We note that the imaginary part of the angular frequency  $\omega_I$  of the gravitational wave perturbation approaches zero from positive value in the extremal limit [40]. This means that the near-extremal over-spinning Kerr geometry, which we deal with in this paper, turns out to be effectively marginally stable. Further it remains to be investigated whether the overspinning geometries arising in the context of string theory via non-trivial ways are unstable to the perturbations. The high energy completion of the Kerr naked singular geometry could stabilize it against the perturbations.

In this paper, we consider the collisional Penrose process in the overspinning Kerr geometry with the spin parameter  $a$  transcending the extremal value  $M$  by a small amount, i.e.,  $a = M(1 + \epsilon)$ , where we take the limit  $\epsilon \rightarrow 0^+$ . Here  $a$  is assumed to be positive without loss of generality. We show that it is necessary for the center-of-mass energy of the colliding particles to diverge in order for the efficiency of the collisional Penrose process to diverge. We had investigated the process of

ultra-high-energy particle collisions in the over-spinning Kerr geometry, wherein the ingoing and outgoing particles, both with the finite radial velocity, collide at  $r = M$  with the divergent center-of-mass energies in the near-extremal limit [41],[42]. An initially ingoing particle starting from the distant location enters the circle  $r = M$  and then turns back as an outgoing particle at the lower radial coordinate if its angular momentum is in the appropriate range. Thus, the outgoing particle that participates in the collision arises naturally in the overspinning Kerr geometry. Many of the drawbacks associated with the process of ultra-high-energy collision in the Kerr black hole case are circumvented. The finetuning of the geodesic parameters of the colliding particles is not required [41]. The time required for the collision is significantly reduced [43]. The upper bound on the center-of-mass energy due to the conservative backreaction of the colliding particles is significantly higher [44]. The escape fraction of the colliding particles is finite [45].

We consider a process where two colliding particles scatter and produce two massless particles. All particles are assumed to move along the equatorial plane for simplicity. It allows us to carry out fully analytical calculations. We choose to work in the center-of-mass tetrad. Since the cross section of the particle physics processes is computed in the center-of-mass frame, it makes the analysis of escape fraction and spectrum of the massless particle easier [24]. The colliding particles travel in the opposite directions in the center-of-mass frame and so do the massless particles which are produced in the collision. The direction along which the massless particles travel can be oriented at any angle with respect to the direction along which colliding particles travel in the center-of-mass frame. However, the angular distribution of massless particles is dictated by the cross section of the underlying particle physics process. We compute the conserved energy of the massless particle as a function of this angle. If a particle escapes to infinity, its conserved energy would be the energy as measured by a distant observer. By analyzing the geodesic motion, we determine the escape cones within which the massless particles must be emitted so that it reaches infinity. The escape cones span half of the angular range. We show that the particle emitted along almost all the directions within the escape cones reaches infinity with divergent energy. The massless particle which travels in the opposite direction with respect to the ultra-high-energy particle that escapes to infinity, has a conserved energy which is negative and also divergent. This implies that the collisional Penrose process is at work and its efficiency shows divergence. It is possible to create ultra-high-energy particles by extracting a large energy from the over-spinning Kerr geometry. Interestingly, the results we obtain here do not depend on whether the center-of-mass frame moves radially inwards, radially outwards or has a zero radial velocity, unlike in the black hole case[28].

All ultra-high-energy massless particles produced in the high-energy collisions have positive an-

gular momenta and almost identical value of the impact parameter. Thus, they co-rotate with the singularity. As seen by the distant observer, they seem to appear from a bright spot located at the specific angular location on that side of the singularity which is rotating towards the observer. We compute the spectrum of the massless particles with the assumptions of the uniform distribution for the angular momenta of the colliding particles and the cross section for the scattering process being constant at large center-of-mass energies. The spectrum admits an upper cut-off energy which can however go to infinity in the near-extremal limit. We consider two cases where the distribution of the massless particles is isotropic in the center-of-mass frame and the case where it is anisotropic. We show that the anisotropy leaves a distinct imprint on the spectrum. Since anisotropy is determined by the differential cross section of the underlying particle physics process, the observation of the spectrum will allow us to put constraints on and distinguish different particle physics models and serve as a probe into fundamental physics at high energies at which particles collide. Thus, the existence of the near-extremal overspinning Kerr spacetime geometry in the Universe, either as a transient configuration or permanent configuration, would have deep implications for astrophysics as well as fundamental particle physics.

When the backreaction is taken into account we expect that the over-spinning Kerr geometry would be driven towards the extremal Kerr black hole configuration. The calculation we present in this paper is meaningful so long as the final spin parameter is larger than the extremal value. This would put an upper bound on the energy of the massless particle. We demonstrate that the upper bound is still so high that it can be of great interest from astrophysical and particle physics point of view.

Interestingly the possibility of production of particle with large conserved energy was briefly mentioned in [46]. We however note that the production of particle with large conserved energy by itself does not imply the large efficiency of collisional Penrose process. Additionally one must ensure that the particle with large conserved energy escapes to infinity, which may not always be the case. One should also demonstrate that the colliding particles must occur naturally, e.g., starting from rest at infinity. This requires the assertion on the global behavior of the metric functions as opposed to the local analysis presented in the paper above. In this paper we carry out an in depth analysis demonstrating that the colliding particles occur naturally, collision results in the production of the particle with large conserved energy and this particle indeed escapes to infinity.

## II. COLLISIONAL PENROSE PROCESS IN GENERAL KERR GEOMETRY

In this section we describe the method we employ to analyze the collisional Penrose process. We keep our discussion general and deal with the Kerr spacetime with an arbitrary spin parameter. Later on we specialize to the overspinning Kerr geometry. We find it convenient to make a transition to the center-of-mass tetrad since the cross section of the particle physics processes is specified in the center-of-mass frame which makes the calculation of escape fraction and energy distribution of the particles produced in the collision easier. Initially, we move over to the locally non-rotating frame (LNRF) and then specify a Lorentz transformation that relates LNRF and center-of-mass frame.

### A. Kerr metric and geodesics in Kerr spacetime

The Kerr metric in the Boyer-Lindquist coordinate system  $(t, r, \theta, \phi)$  is given by

$$ds^2 = - \left( 1 - \frac{2Mr}{\Sigma} \right) dt^2 + \left( r^2 + a^2 + \frac{2Mra^2}{\Sigma} \sin^2 \theta \right) \sin^2 \theta d\phi^2 - \frac{2Mra}{\Sigma} \sin^2 \theta dt d\phi + \frac{\Sigma}{\Delta} dr^2 + \Sigma d\theta^2, \quad (1)$$

where  $\Delta = (r^2 - 2Mr + a^2)$  and  $\Sigma = (r^2 + a^2 \cos^2 \theta)$ . The Kerr metric contains two parameters, namely mass  $M$  and spin parameter  $a = J/M$  where  $J$  is the angular momentum. Without the loss of generality we assume that the spin parameter  $a$  is positive. When  $a \leq M$ , the Kerr metric describes a rotating black hole. A Kerr black hole is said to be extremal if the spin parameter admits the maximum permissible value  $a = M$ . The event horizon for the extremal black hole is located at  $r = M$ . If we go past the extremality, i.e., for the spin parameter larger than the mass  $a > M$ , the event horizon is absent and spacetime admits a rotating naked singularity at  $r = 0$  in the equatorial plane. The Kerr spacetime admits two Killing vectors, namely a timelike Killing vector  $k = \partial_t$  and azimuthal Killing vector  $l = \partial_\phi$  that correspond to the time translation and rotational invariance, respectively, which is evident from the fact that the Kerr metric (1) is independent of the  $t$  and  $\phi$ .

Consider a massive particle following a geodesic motion on the equatorial plane of the Kerr

spacetime. The four-velocity of such a particle in the Boyer-Lindquist coordinates is given by

$$\begin{aligned}
U^t &= \frac{1}{\Delta} \left( E \left( r^2 + a^2 + \frac{2Ma^2}{r} \right) - \frac{2Ma}{r} L \right) , \\
U^\phi &= \frac{1}{\Delta} \left( \frac{2Ma}{r} E + \left( 1 - \frac{2M}{r} \right) L \right) , \\
U^r &= \sigma \sqrt{E^2 - 1 + \frac{2M}{r} - \frac{L^2 - a^2 (E^2 - 1)}{r^2} + \frac{2M (L - aE)^2}{r^3}} , \\
U^\theta &= 0 ,
\end{aligned} \tag{2}$$

where  $E = -k \cdot U$  is the conserved energy per unit mass and  $L = l \cdot U$  is the conserved angular momentum per unit mass of the particle. These are the constants of motion associated with the time translation and rotational symmetry. The components of four-velocity (2) are obtained by solving the equations that define the conserved quantities  $E = -k \cdot U$ ,  $L = l \cdot U$  and the normalization condition for velocity  $U \cdot U = -1$ . We have  $\sigma = \pm 1$  for radially outgoing and ingoing particles, respectively.

We now consider a massless particle following a geodesic motion on the equatorial plane. The four-velocity components of the massless particles moving on the equatorial plane are given by

$$\begin{aligned}
U^t &= \frac{1}{\Delta} \left( \left( r^2 + a^2 + \frac{2Ma^2}{r} \right) - \frac{2Mab}{r} \right) , \\
U^\phi &= \frac{1}{\Delta} \left( \frac{2Ma}{r} + \left( 1 - \frac{2M}{r} \right) b \right) , \\
U^r &= \sigma \sqrt{1 - \frac{(b^2 - a^2)}{r^2} + \frac{2M(b - a)^2}{r^3}} , \\
U^\theta &= 0 ,
\end{aligned} \tag{3}$$

where  $b = L/E$  is an impact parameter with  $E$  as conserved energy and  $L$  as angular momentum of the massless particle, which are the constants of motion associated with time translational and rotational invariance of the Kerr metric, respectively. The components for four-velocity are obtained by solving the equations for the conserved quantities  $E = -k \cdot U$ ,  $L = l \cdot U$  and the normalization condition for velocity of massless particle  $U \cdot U = 0$  and then changing the parametrization  $\lambda \rightarrow E\lambda$ .

Note that  $E$  and  $L$  are conserved energy and angular momentum per unit mass for massive particle, respectively, whereas they also stand for conserved energy and angular momentum for massless particle.

## B. LNRF

One of the most remarkable features of the Kerr metric is the phenomenon of frame-dragging, i.e., spacetime drags geodesics sideways in the azimuthal direction in the same direction as that of the rotation. It can be inferred from Eqs. (2) and (3) as even the particle with the zero angular momentum acquires positive angular velocity when it falls radially inwards.

A locally non-rotating frame (LNRF) is the tetrad associated with an observer who executes a circular motion at a constant radial coordinate with the frequency associated with frame-dragging. Restricting to the equatorial plane, the components of LNRF basis one-forms are given by

$$\begin{aligned}
e_{\mu}^{(t)} & : e_t^{(t)} = \sqrt{\frac{\Delta}{(r^2 + a^2 + \frac{2M}{r}a^2)}} ; e_{\phi}^{(t)} = 0 ; e_r^{(t)} = 0 ; e_{\theta}^{(t)} = 0 , \\
e_{\mu}^{(\phi)} & : e_t^{(\phi)} = -\frac{\frac{2Ma}{r}}{\sqrt{(r^2 + a^2 + \frac{2Ma^2}{r})}} ; e_{\phi}^{(\phi)} = \sqrt{(r^2 + a^2 + \frac{2Ma^2}{r})} ; e_r^{(\phi)} = 0 ; e_{\theta}^{(\phi)} = 0 , \\
e_{\mu}^{(r)} & : e_t^{(r)} = 0 ; e_{\phi}^{(r)} = 0 ; e_r^{(r)} = \frac{r}{\sqrt{\Delta}} ; e_{\theta}^{(r)} = 0 , \\
e_{\mu}^{(\theta)} & : e_t^{(\theta)} = 0 ; e_{\phi}^{(\theta)} = 0 ; e_r^{(\theta)} = 0 ; e_{\theta}^{(\theta)} = \sqrt{(r^2 + a^2 + \frac{2Ma^2}{r})} .
\end{aligned} \tag{4}$$

We now make a transition to the LNRF. We intend to work in the center-of-mass tetrad as it makes computation of the spectrum and escape fraction easier. Since the two tetrads are related to each other by a Lorentz transformation it would be convenient to make a transition to the auxiliary intermediate tetrad from the Boyer-Lindquist coordinates and then figure out the requisite Lorentz transformation that would take us from intermediate tetrad to the center of mass frame. We choose auxiliary intermediate tetrad to be the locally non-rotating frame (4). Components of an arbitrarily vector  $V$  transform in the following way as we make a transition from Boyer-Lindquist to LNRF

$$V_{LNRF}^{(\mu)} = e_{\nu}^{(\mu)} V^{\nu} . \tag{5}$$

Thus , Eqs. (2), (4) and (5) , the components of velocity of the massive particle in LNRF are given

by

$$\begin{aligned}
U_{LNRF}^{(t)} &= \frac{1}{\sqrt{\Delta}} \frac{\left(E \left(r^2 + a^2 + \frac{2Ma^2}{r}\right) - \frac{2Ma}{r} L\right)}{\sqrt{\left(r^2 + a^2 + \frac{2Ma^2}{r}\right)}}, \\
U_{LNRF}^{(\phi)} &= \frac{L}{\sqrt{\left(r^2 + a^2 + \frac{2Ma^2}{r}\right)}}, \\
U_{LNRF}^{(r)} &= \sigma \frac{r}{\sqrt{\Delta}} \sqrt{E^2 - 1 + \frac{2M}{r} - \frac{L^2 - a^2(E^2 - 1)}{r^2} + \frac{2M(L - aE)^2}{r^3}}, \\
U_{LNRF}^{(\theta)} &= 0, \tag{6}
\end{aligned}$$

and components for the velocity of the massless particle obtained from Eqs. (3), (4) and (5) are given by

$$\begin{aligned}
U_{LNRF}^{(t)} &= \frac{1}{\sqrt{\Delta}} \frac{\left(\left(r^2 + a^2 + \frac{2Ma^2}{r}\right) - \frac{2Mab}{r}\right)}{\sqrt{\left(r^2 + a^2 + \frac{2Ma^2}{r}\right)}}, \\
U_{LNRF}^{(\phi)} &= \frac{b}{\sqrt{\left(r^2 + a^2 + \frac{2Ma^2}{r}\right)}}, \\
U_{LNRF}^{(r)} &= \sigma \frac{r}{\sqrt{\Delta}} \sqrt{1 - \frac{(b^2 - a^2)}{r^2} + \frac{2M(b - a)^2}{r^3}}, \\
U_{LNRF}^{(\theta)} &= 0. \tag{7}
\end{aligned}$$

We consider a collision between two identical massive particles that follow a geodesic motion of the equatorial plane each with mass  $m$  at a radial coordinate  $r$ . Let the conserved energy per unit mass and angular momentum per unit mass for two particles be  $E_i$  and  $L_i$  with  $i = 1, 2$ , respectively. It is a priori unspecified whether the particles are radially ingoing or outgoing  $\sigma_i = \pm$ . As we describe later we choose one of the colliding particles to be radially ingoing and other particle to be radially outgoing. The components of the velocity of the colliding particles in the LNRF can be obtained from Eq. (6) simply by putting subscript  $i$  on various relevant quantities as  $U_{i,LNRF}^{(\mu)}$ ,  $E_i$ ,  $L_i$  and  $\sigma_i$ .

We find it convenient to define the quantities  $A$ ,  $B$  and  $C$ , which can be interpreted as non-zero components of the net velocity of the two colliding particles in LNRF. They would appear in this

paper multiple times at various places. While  $A$  is always positive for future pointing velocity vectors,  $B$  and  $C$  can be positive or negative. Results can be qualitatively different depending on whether  $B$  and  $C$  are positive or negative. We analyze these cases separately.

From Eq. (6) we write the expressions for  $A$ ,  $B$  and  $C$ :

$$\begin{aligned}
A &= U_{1,LNRF}^{(t)} + U_{2,LNRF}^{(t)} \\
&= \frac{1}{\sqrt{\Delta}} \frac{\left(E_1 \left(r^2 + a^2 + \frac{2Ma^2}{r}\right) - \frac{2Ma}{r} L_1\right)}{\sqrt{\left(r^2 + a^2 + \frac{2Ma^2}{r}\right)}} + \frac{1}{\sqrt{\Delta}} \frac{\left(E_2 \left(r^2 + a^2 + \frac{2Ma^2}{r}\right) - \frac{2Ma}{r} L_2\right)}{\sqrt{\left(r^2 + a^2 + \frac{2Ma^2}{r}\right)}}, \\
B &= U_{1,LNRF}^{(r)} + U_{2,LNRF}^{(r)} \\
&= \sigma_1 \frac{r}{\sqrt{\Delta}} \sqrt{E_1^2 - 1 + \frac{2M}{r} - \frac{L_1^2 - a^2 (E_1^2 - 1)}{r^2} + \frac{2M (L_1 - aE_1)^2}{r^3}} \\
&\quad + \sigma_2 \frac{r}{\sqrt{\Delta}} \sqrt{E_2^2 - 1 + \frac{2M}{r} - \frac{L_2^2 - a^2 (E_2^2 - 1)}{r^2} + \frac{2M (L_2 - aE_2)^2}{r^3}}, \\
C &= U_{1,LNRF}^{(\phi)} + U_{2,LNRF}^{(\phi)} \\
&= \frac{L_1}{\sqrt{\left(r^2 + a^2 + \frac{2Ma^2}{r}\right)}} + \frac{L_2}{\sqrt{\left(r^2 + a^2 + \frac{2Ma^2}{r}\right)}}. \tag{8}
\end{aligned}$$

If  $B > 0$ , then the net radial velocity of the two particles in LNRF is positive, which implies the center of mass of the two colliding particles moves in the radially outward direction from the point of view of LNRF frame as well as Boyer-Lindquist coordinate system since the sign of the radial velocity does not change as one makes a transition from the Boyer-Lindquist to LNRF. When  $B < 0$ , the center of mass travels in the radially inward direction and when  $B = 0$ , the center of mass does not move along the radial direction. The sign of  $C$  depicts whether the center of mass is co-rotating or counter-rotating with respect to the spacetime rotation.

### C. Center-of-mass frame

We now make a transition to the center-of-mass frame. It can be achieved by means of an appropriate Lorentz transformation relating the LNRF and the center of mass frame. The Lorentz transformation is split into two parts. A rotation that orients the spatial part of the net velocity of the two colliding particles in the radial direction and a boost in the radial direction that kills the radial component of the net velocity. In the center-of-mass frame the net velocity of the two particles has all spatial components zero.

We now write down the transformation that relates the components of any arbitrary vector  $V$  in the LNRF to the components in the center-of-mass frame

$$V_{cm}^{(\mu)} = \Lambda_{boost\ \nu}^{\mu} \Lambda_{rot\ \sigma}^{\nu} V_{LNRF}^{(\sigma)} = \Lambda_{boost\ \nu}^{\mu} \Lambda_{rot\ \sigma}^{\nu} e_{\delta}^{(\sigma)} V^{\delta} , \quad (9)$$

where the transformation  $\Lambda_{rot\ \sigma}^{\nu}$  appearing in the equation above implements following rotation:

$$\begin{aligned} V_{rot}^{(t)} &= V_{LNRF}^{(t)} , \\ V_{rot}^{(r)} &= \frac{B}{\sqrt{B^2 + C^2}} V_{LNRF}^{(r)} + \frac{C}{\sqrt{B^2 + C^2}} V_{LNRF}^{(\phi)} , \\ V_{rot}^{(\phi)} &= -\frac{C}{\sqrt{B^2 + C^2}} V_{LNRF}^{(r)} + \frac{B}{\sqrt{B^2 + C^2}} V_{LNRF}^{(\phi)} , \\ V_{rot}^{(\theta)} &= V_{LNRF}^{(\theta)} , \end{aligned} \quad (10)$$

and the transformation  $\Lambda_{boost\ \nu}^{\mu}$  implements the following boost:

$$\begin{aligned} V_{cm}^{(t)} &= \frac{A}{\sqrt{A^2 - B^2 - C^2}} V_{rot}^{(t)} - \frac{\sqrt{B^2 + C^2}}{\sqrt{A^2 - B^2 - C^2}} V_{rot}^{(r)} , \\ V_{cm}^{(r)} &= -\frac{\sqrt{B^2 + C^2}}{\sqrt{A^2 - B^2 - C^2}} V_{rot}^{(t)} + \frac{A}{\sqrt{A^2 - B^2 - C^2}} V_{rot}^{(r)} , \\ V_{cm}^{(\phi)} &= V_{rot}^{(\phi)} , \\ V_{cm}^{(\theta)} &= V_{rot}^{(\theta)} . \end{aligned} \quad (11)$$

We now write down the components of velocity of the massive particle in the center of mass frame. From Eqs. (6), (9), (10) and (11) we obtain

$$\begin{aligned} U_{cm}^{(t)} &= \frac{A}{\sqrt{A^2 - B^2 - C^2}} \frac{1}{\sqrt{\Delta}} \frac{\left( \left( r^2 + a^2 + \frac{2Ma^2}{r} \right) E - \frac{2MaL}{r} \right)}{\sqrt{\left( r^2 + a^2 + \frac{2Ma^2}{r} \right)}} - \frac{C}{\sqrt{A^2 - B^2 - C^2}} \frac{L}{\sqrt{\left( r^2 + a^2 + \frac{2Ma^2}{r} \right)}} \\ &\quad - \frac{B}{\sqrt{A^2 - B^2 - C^2}} \sigma \frac{r}{\sqrt{\Delta}} \sqrt{E^2 - 1 + \frac{2M}{r} - \frac{L^2 - a^2(E^2 - 1)}{r^2} + \frac{2M(L - aE)^2}{r^3}} , \end{aligned}$$

$$\begin{aligned}
U_{cm}^{(r)} &= -\frac{\sqrt{B^2 + C^2}}{\sqrt{A^2 - B^2 - C^2}} \frac{1}{\sqrt{\Delta}} \frac{\left( \left( r^2 + a^2 + \frac{2Ma^2}{r} \right) E - \frac{2MaL}{r} \right)}{\sqrt{\left( r^2 + a^2 + \frac{2Ma^2}{r} \right)}} \\
&\quad + \frac{AC}{\sqrt{A^2 - B^2 - C^2} \sqrt{B^2 + C^2}} \frac{L}{\sqrt{\left( r^2 + a^2 + \frac{2Ma^2}{r} \right)}} \\
&\quad + \frac{AB}{\sqrt{A^2 - B^2 - C^2} \sqrt{B^2 + C^2}} \sigma \frac{r}{\sqrt{\Delta}} \sqrt{E^2 - 1 + \frac{2M}{r} - \frac{L^2 - a^2(E^2 - 1)}{r^2} + \frac{2M(L - aE)^2}{r^3}}, \\
U_{cm}^{(\phi)} &= -\frac{C}{\sqrt{B^2 + C^2}} \sigma \frac{r}{\sqrt{\Delta}} \sqrt{E^2 - 1 + \frac{2M}{r} - \frac{L^2 - a^2(E^2 - 1)}{r^2} + \frac{2M(L - aE)^2}{r^3}} \\
&\quad + \frac{B}{\sqrt{B^2 + C^2}} \frac{L}{\sqrt{\left( r^2 + a^2 + \frac{2Ma^2}{r} \right)}}, \\
U_{cm}^{(\theta)} &= 0.
\end{aligned} \tag{12}$$

The components of the velocity for the massless particle in the center-of-mass frame can be obtained from Eqs. (7), (9), (10) and (11) and are given by

$$\begin{aligned}
U_{cm}^{(t)} &= \frac{A}{\sqrt{A^2 - B^2 - C^2}} \frac{1}{\sqrt{\Delta}} \frac{\left( \left( r^2 + a^2 + \frac{2Ma^2}{r} \right) - \frac{2Mab}{r} \right)}{\sqrt{\left( r^2 + a^2 + \frac{2Ma^2}{r} \right)}} - \frac{C}{\sqrt{A^2 - B^2 - C^2}} \frac{b}{\sqrt{\left( r^2 + a^2 + \frac{2Ma^2}{r} \right)}} \\
&\quad - \frac{B}{\sqrt{A^2 - B^2 - C^2}} \sigma \frac{r}{\sqrt{\Delta}} \sqrt{1 - \frac{(b^2 - a^2)}{r^2} + \frac{2M(b - a)^2}{r^3}}, \\
U_{cm}^{(r)} &= -\frac{\sqrt{B^2 + C^2}}{\sqrt{A^2 - B^2 - C^2}} \frac{1}{\sqrt{\Delta}} \frac{\left( \left( r^2 + a^2 + \frac{2Ma^2}{r} \right) - \frac{2Mab}{r} \right)}{\sqrt{\left( r^2 + a^2 + \frac{2Ma^2}{r} \right)}} \\
&\quad + \frac{AC}{\sqrt{A^2 - B^2 - C^2} \sqrt{B^2 + C^2}} \frac{b}{\sqrt{\left( r^2 + a^2 + \frac{2Ma^2}{r} \right)}} \\
&\quad + \frac{AB}{\sqrt{A^2 - B^2 - C^2} \sqrt{B^2 + C^2}} \sigma \frac{r}{\sqrt{\Delta}} \sqrt{1 - \frac{(b^2 - a^2)}{r^2} + \frac{2M(b - a)^2}{r^3}}, \\
U_{cm}^{(\phi)} &= -\frac{C}{\sqrt{B^2 + C^2}} \sigma \frac{r}{\sqrt{\Delta}} \sqrt{1 - \frac{(b^2 - a^2)}{r^2} + \frac{2M(b - a)^2}{r^3}} \\
&\quad + \frac{B}{\sqrt{B^2 + C^2}} \frac{b}{\sqrt{\left( r^2 + a^2 + \frac{2Ma^2}{r} \right)}}, \\
U_{cm}^{(\theta)} &= 0.
\end{aligned} \tag{13}$$

#### D. Collision as seen from the center-of-mass frame

We now provide a description of the collision event in the center-of-mass frame. As stated earlier we choose to work in the center-of-mass frame because the differential cross section of the underlying particle physics process is computed in the center-of-mass frame. It tells us whether the emission of collision products is isotropic or anisotropic in the center-of-mass frame which is the crucial ingredient required to infer the shape of the energy distribution function of the particles escaping to infinity. Thus, from the point of view of calculation of the observables, it is convenient to work in the center-of-mass frame.

As mentioned earlier, we consider collision between two identical massive particles which we refer to as particle 1 and particle 2. The colliding particles travel in the opposite directions in the center-of-mass frame with equal and opposite velocity. This can be inferred easily by computing the components of net velocity of the colliding particles in the center-of-mass frame. From Eqs. (8) and (12) we obtain

$$U_{1,cm}^{(\alpha)} + U_{2,cm}^{(\alpha)} = \sqrt{A^2 - B^2 - C^2}(1, 0, 0, 0). \quad (14)$$

The spatial components of net velocity are zero. The time component of the net velocity yields the center-of-mass energy of collision  $E_{cm}$  when multiplied by the mass  $m$  of the colliding particles

$$E_{cm} = m \left( U_{1,cm}^{(t)} + U_{2,cm}^{(t)} \right) = m \sqrt{A^2 - B^2 - C^2}. \quad (15)$$

We assume that two massless particles are produced in the collision which we refer to as particle 3 and particle 4. In this paper we focus on the massless particles that move only along the equatorial plane. The most general expression for the components of the momenta of the two massless particles  $P_3$  and  $P_4$  moving on the equatorial plane can be written as

$$P_{3,cm}^\mu = m \frac{\sqrt{A^2 - B^2 - C^2}}{2} (1, \cos \alpha, \sin \alpha, 0), \quad (16)$$

and

$$P_{4,cm}^\mu = m \frac{\sqrt{A^2 - B^2 - C^2}}{2} (1, -\cos \alpha, -\sin \alpha, 0), \quad (17)$$

respectively. It can be easily verified from the expressions above that  $P_3$  and  $P_4$  are consistent with energy-momentum conservation  $P_{3,cm}^{(\mu)} + P_{4,cm}^{(\mu)} = m \left( U_{1,cm}^{(\mu)} + U_{2,cm}^{(\mu)} \right)$  and are null vectors  $\eta_{\mu\nu} P_{3,cm}^{(\mu)} P_{3,cm}^{(\nu)} = \eta_{\mu\nu} P_{4,cm}^{(\mu)} P_{4,cm}^{(\nu)} = 0$ . Further it is quite clear from the transformation Eqs. (9), (4), (10) and (11) from the Boyer-Lindquist coordinate system to LNRF and Eqs. (16)

and (17) that  $P_3^{(\theta)} = P_4^{(\theta)} = 0$ . Thus, particles move on the equatorial plane. In the center-of-mass frame particles move in the  $\hat{r} - \hat{\phi}$  plane. The parameter  $\alpha$  which appears in Eqs. (16) and (17) can be interpreted as the angle between the direction in which particle 3 travels and  $\hat{r}$  direction. Whereas particle 4 travels along the direction which makes angle  $\pi + \alpha$  with  $\hat{r}$ . The particles travel along opposite directions with equal and opposite momenta in the center of mass frame.

We now compute the conserved energies and angular momenta of the two massless particles produced in the collision. We write down the components of the timelike Killing vector  $k$  and azimuthal Killing vector  $l$  in the center-of-mass frame. Their components in the Boyer-Lindquist coordinate system are

$$\begin{aligned} k^\mu &= (1, 0, 0, 0) , \\ l^\mu &= (0, 0, 1, 0) . \end{aligned} \tag{18}$$

From Eqs. (18), (9), (4), (10) and (11), the components of the timelike Killing vector in the center-of-mass frame can be written as

$$\begin{aligned} k_{cm}^{(t)} &= \frac{A}{\sqrt{A^2 - B^2 - C^2}} \sqrt{\frac{\Delta}{\left(r^2 + a^2 + \frac{2Ma^2}{r}\right)}} + \frac{C}{\sqrt{A^2 - B^2 - C^2}} \frac{\frac{2Ma}{r}}{\sqrt{r^2 + a^2 + \frac{2Ma^2}{r}}} , \\ k_{cm}^{(r)} &= -\frac{\sqrt{B^2 + C^2}}{\sqrt{A^2 - B^2 - C^2}} \sqrt{\frac{\Delta}{\left(r^2 + a^2 + \frac{2Ma^2}{r}\right)}} - \frac{AC}{\sqrt{A^2 - B^2 - C^2}} \frac{\frac{2Ma}{r}}{\sqrt{B^2 + C^2}} , \\ k_{cm}^{(\phi)} &= -\frac{B}{\sqrt{B^2 + C^2}} \frac{\frac{2Ma}{r}}{\sqrt{\left(r^2 + a^2 + \frac{2Ma^2}{r}\right)}} , \\ k_{cm}^{(\theta)} &= 0 , \end{aligned} \tag{19}$$

and the components of azimuthal Killing vector are given by

$$\begin{aligned} l_{cm}^{(t)} &= -\frac{C}{\sqrt{A^2 - B^2 - C^2}} \sqrt{\frac{\Delta}{\left(r^2 + a^2 + \frac{2Ma^2}{r}\right)}} , \\ l_{cm}^{(r)} &= \frac{AC}{\sqrt{A^2 - B^2 - C^2}} \frac{\sqrt{\left(r^2 + a^2 + \frac{2Ma^2}{r}\right)}}{\sqrt{B^2 + C^2}} , \\ l_{cm}^{(\phi)} &= \frac{B}{\sqrt{B^2 + C^2}} \sqrt{\left(r^2 + a^2 + \frac{2Ma^2}{r}\right)} , \\ l_{cm}^{(\theta)} &= 0 . \end{aligned} \tag{20}$$

The conserved energies  $E_i$  and angular momenta  $L_i$  are obtained by taking the inner product of the timelike and azimuthal Killing vectors with the momentum vectors of the two particles produced in

the collision. The components of all the relevant quantities are written down in the center-of-mass frame. From Eqs. (16), (17), (19) and (20), the conserved energies of the massless particles  $E_3$  and  $E_4$  are given by

$$\begin{aligned}
E_3 &= -\eta_{\mu\nu} P_{3,cm}^{(\mu)} k_{cm}^{(\nu)} \\
&= \frac{m}{2} \frac{\sqrt{\Delta} A + \frac{2Ma}{r} C}{\sqrt{\left(r^2 + a^2 + \frac{2Ma^2}{r}\right)}} + \frac{m}{2} \frac{\sqrt{\Delta} \sqrt{B^2 + C^2} + \frac{2Ma}{r} \frac{AC}{\sqrt{B^2 + C^2}}}{\sqrt{\left(r^2 + a^2 + \frac{2Ma^2}{r}\right)}} \cos \alpha \\
&\quad + \frac{m}{2} \frac{\frac{2Ma}{r}}{\sqrt{\left(r^2 + a^2 + \frac{2Ma^2}{r}\right)}} \frac{B}{\sqrt{B^2 + C^2}} \sqrt{A^2 - B^2 - C^2} \sin \alpha, \tag{21}
\end{aligned}$$

and

$$\begin{aligned}
E_4 &= -\eta_{\mu\nu} P_{4,cm}^{(\mu)} k_{cm}^{(\nu)} \\
&= \frac{m}{2} \frac{\sqrt{\Delta} A + \frac{2Ma}{r} C}{\sqrt{\left(r^2 + a^2 + \frac{2Ma^2}{r}\right)}} - \frac{m}{2} \frac{\sqrt{\Delta} \sqrt{B^2 + C^2} + \frac{2Ma}{r} \frac{AC}{\sqrt{B^2 + C^2}}}{\sqrt{\left(r^2 + a^2 + \frac{2Ma^2}{r}\right)}} \cos \alpha \\
&\quad - \frac{m}{2} \frac{\frac{2Ma}{r}}{\sqrt{\left(r^2 + a^2 + \frac{2Ma^2}{r}\right)}} \frac{B}{\sqrt{B^2 + C^2}} \sqrt{A^2 - B^2 - C^2} \sin \alpha, \tag{22}
\end{aligned}$$

respectively, and angular momenta  $L_3$  and  $L_4$  can be written as

$$\begin{aligned}
L_3 &= \eta_{\mu\nu} P_{3,cm}^{(\mu)} l_{cm}^{(\nu)} \\
&= \frac{m}{2} \sqrt{\left(r^2 + a^2 + \frac{2Ma^2}{r}\right)} C + \frac{m}{2} \sqrt{\left(r^2 + a^2 + \frac{2Ma^2}{r}\right)} \frac{AC}{\sqrt{B^2 + C^2}} \cos \alpha \\
&\quad + \frac{m}{2} \sqrt{\left(r^2 + a^2 + \frac{2Ma^2}{r}\right)} \frac{B}{\sqrt{B^2 + C^2}} \sqrt{A^2 - B^2 - C^2} \sin \alpha, \tag{23}
\end{aligned}$$

and

$$\begin{aligned}
L_4 &= \eta_{\mu\nu} P_{4,cm}^{(\mu)} l_{cm}^{(\nu)} \\
&= \frac{m}{2} \sqrt{\left(r^2 + a^2 + \frac{2Ma^2}{r}\right)} C - \frac{m}{2} \sqrt{\left(r^2 + a^2 + \frac{2Ma^2}{r}\right)} \frac{AC}{\sqrt{B^2 + C^2}} \cos \alpha \\
&\quad - \frac{m}{2} \sqrt{\left(r^2 + a^2 + \frac{2Ma^2}{r}\right)} \frac{B}{\sqrt{B^2 + C^2}} \sqrt{A^2 - B^2 - C^2} \sin \alpha, \tag{24}
\end{aligned}$$

respectively.

If the massless particle produced in the collision escapes to infinity, then its conserved energy is the energy of the particle as measured by the asymptotic observer. Thus, no further effort is required to infer the energy of the massless particle measured at infinity than to specify the

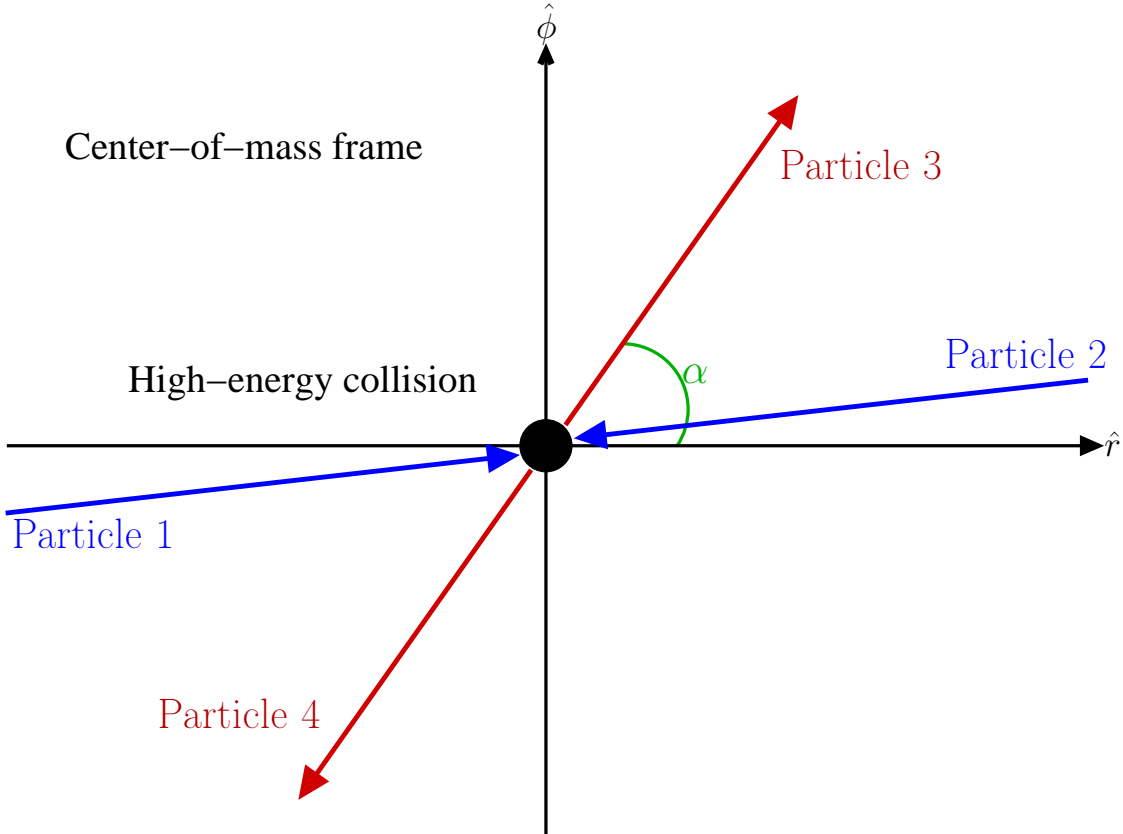


FIG. 1: Collision as seen from the center-of-mass tetrad. Two massive particles, namely particle 1 and particle 2, collide and produce two massless particles, namely particle 3 and particle 4. All particles travel in  $\hat{r} - \hat{\phi}$  plane in the center-of-mass frame. The colliding particles as well as collision products travel in the opposite direction with equal and opposite momenta. Particle 3 travels along the direction which makes angle  $\alpha$  with  $\hat{r}$ .

direction along which it is emitted in the center-of-mass frame. We must determine the directions along which the particle must be emitted in the center-of-mass frame so that it escapes to infinity. Without the loss of generality we label the particle which escapes to infinity as particle 3.

### E. Conditions for the massless particle to escape to infinity

We now derive the conditions necessary for the massless particle produced in the collision to escape to infinity. Consider a massless particle with an impact parameter  $b$  following a geodesic motion on the equatorial plane of the Kerr spacetime. The radial component of velocity in the

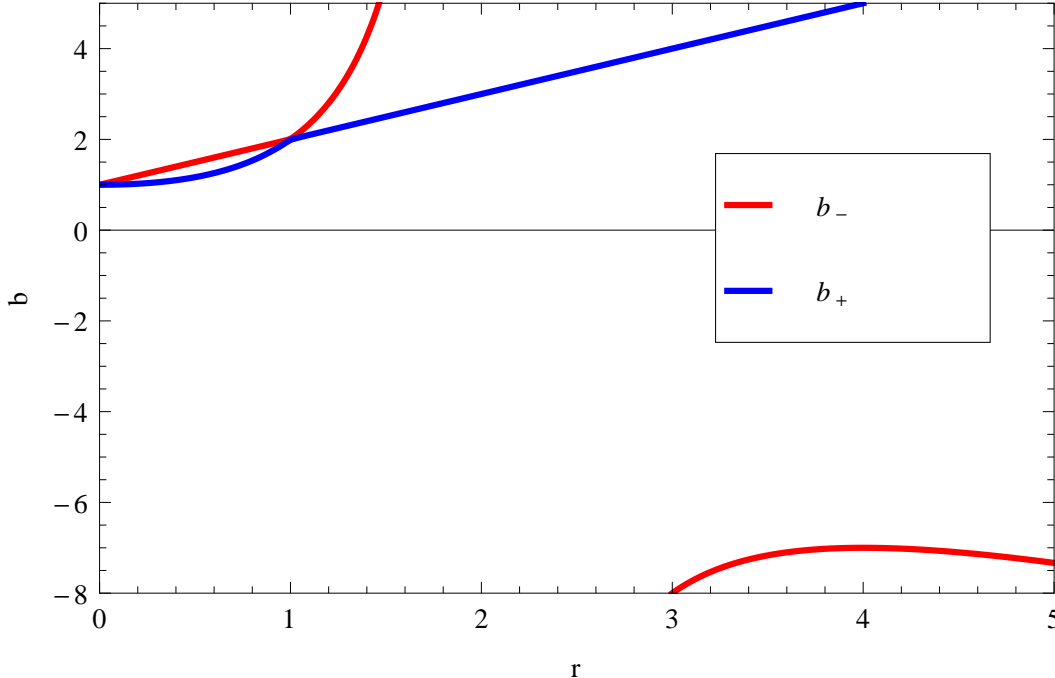


FIG. 2: The impact parameter  $b(r)$  required for the massless particles to admit a turning point at a radial coordinate  $r$  is plotted here. Both  $b$  and  $r$  are expressed in units of  $M$ .  $b$  admits two branches,  $b_-$  denoted by red curve and  $b_+$  denoted by blue curve. The Kerr spin parameter is taken to be  $a = 1.0001M$ .

Boyer-Lindquist coordinate system can be read off from Eq. (3) as

$$U^r = \pm \sqrt{1 - \frac{(b^2 - a^2)}{r^2} + \frac{2M(b - a)^2}{r^3}}. \quad (25)$$

The value that the impact parameter  $b(r)$  must take if it is to admit a turning point at a radial coordinate  $r$ , i.e. for  $U^r = 0$  is given by the expression

$$b_{\pm}(r) = \frac{-2Ma \pm r\sqrt{\Delta}}{(r - 2M)}. \quad (26)$$

The expression above contains the factor  $\sqrt{\Delta}$ . Analysis for the Kerr black hole and the overspinning Kerr geometry must be carried out separately since for the black hole  $\Delta = 0$  at the horizon  $r = r_h$  and the region below horizon  $r < r_h$  is irrelevant for the discussion, whereas in case of the naked singularity  $\Delta$  remains positive throughout the spacetime. Here we focus on the overspinning Kerr geometry since it is relevant from the point of view of results discussed in this paper. An analysis for the Kerr black hole was carried out in [23],[24].

We first analyze the behavior of  $b_+(r)$ . It is a monotonically increasing function which is always positive. At the location of the singularity, i.e., at  $r = 0$ , it takes a value  $b_+(r = 0) = a$ . At

$r = 2M$  both the denominator and numerator vanish in the expression for  $b_+$ . However one can take an appropriate limit and obtain  $b_+(r = 2M) = a + (2M^2/a)$ . As we approach infinity it shows a divergence  $b_+(r \rightarrow \infty) \rightarrow \infty$ .

We now analyze the behavior of  $b_-(r)$ . When  $r < 2M$ ,  $b_-(r)$  is always larger than  $b_+(r)$ , i.e.,  $b_-(r) > b_+(r)$ . At the location of the singularity  $r = 0$ , it takes value  $b_-(r = 0) = a$ . When we approach  $r = 2M$  from left, it goes to plus infinity  $b_-(r \rightarrow 2M^-) \rightarrow +\infty$ . When we approach  $r = 2M$  from right,  $b_-$  goes to negative infinity. For  $r > 2M$ ,  $b_-(r)$  is always negative. The radial coordinate  $r_m$  at which  $b_-$  admits maximum and its maximum value are given by

$$r_m = \frac{M^{\frac{1}{3}} \left( M^{\frac{2}{3}} + \left( a + \sqrt{a^2 - M^2} \right)^{\frac{2}{3}} \right)^2}{\left( a + \sqrt{a^2 - M^2} \right)^{\frac{2}{3}}}; \quad b_-(r = r_m) = a - \frac{\left( M^{\frac{2}{3}} + \left( a + \sqrt{a^2 - M^2} \right)^{\frac{2}{3}} \right)^3}{\left( a + \sqrt{a^2 - M^2} \right)}. \quad (27)$$

As we approach infinity it goes to negative infinity  $b_-(r \rightarrow \infty) \rightarrow -\infty$ . Behavior of  $b_+(r)$  and  $b_-(r)$  is as shown in Fig. 2.

Conditions that must be imposed on the impact parameter of the massless particle created in the collision so that it escapes to infinity are different depending on whether the collision takes place at the location with  $r < r_m$  or  $r > r_m$ .

If the collision occurs at  $r < r_m$  and if the massless particle travels radially inwards, i.e.,  $\sigma = -1$ , then its impact parameter must be in the following range for it to admit a turning point at the lower radius and escape to infinity:

$$r < r_m, \quad \sigma = -1 \quad \implies \quad b \in (a, b_+(r)) . \quad (28)$$

If the massless particle travels radially outwards, i.e.,  $\sigma = +1$ , then its impact parameter must be in the following range for it to escape:

$$r < r_m, \quad \sigma = +1 \quad \implies \quad b \in (b_-(r_m), b_+(r)) . \quad (29)$$

If the collision occurs at  $r > r_m$  and if the massless particle travels radially inwards, i.e.,  $\sigma = -1$ , then its impact parameter must be in the following range for it to turn back at the lower radius and escape to infinity:

$$r > r_m, \quad \sigma = -1 \quad \implies \quad b \in (a, b_+(r)) \cup (b_-(r), b_-(r_m)) . \quad (30)$$

If the massless particle travels radially outwards  $\sigma = +1$ , then its impact parameter must be in the following range for it to escape:

$$r > r_m, \quad \sigma = +1 \quad \implies \quad b \in (b_-(r), b_+(r)) . \quad (31)$$

If these conditions are met, then the massless particle created in the particle collision will escape to infinity.

### F. Escape cones in the center-of-mass frame

We derived the conditions that must be imposed on the impact parameter of the massless particle generated in the collision for it to escape to infinity. We now translate these conditions into the set of directions along which the particle must be emitted in the center-of-mass frame. We compute the escape cones, i.e., the permissible angular range for the escape of the massless particle.

The massless particle moves in the  $\hat{r} - \hat{\phi}$  plane in the center-of-mass frame. The nonzero spatial components of the velocity in the center-of-mass frame can be read off from Eq. (13) and are given by

$$\begin{aligned}
U_{cm}^{(r)} = & \frac{-\sqrt{B^2 + C^2}}{\sqrt{A^2 - B^2 - C^2}} \frac{1}{\sqrt{\Delta}} \frac{\left( \left( r^2 + a^2 + \frac{2Ma^2}{r} \right) - \frac{2Mab}{r} \right)}{\sqrt{\left( r^2 + a^2 + \frac{2Ma^2}{r} \right)}} \\
& + \frac{AB}{\sqrt{A^2 - B^2 - C^2} \sqrt{B^2 + C^2}} \sigma \frac{r}{\sqrt{\Delta}} \sqrt{1 - \frac{(b^2 - a^2)}{r^2} + \frac{2M(b-a)^2}{r^3}} \\
& + \frac{AC}{\sqrt{A^2 - B^2 - C^2} \sqrt{B^2 + C^2}} \frac{b}{\sqrt{\left( r^2 + a^2 + \frac{2Ma^2}{r} \right)}}, \tag{32}
\end{aligned}$$

and

$$\begin{aligned}
U_{cm}^{(\phi)} = & -\frac{C}{\sqrt{B^2 + C^2}} \sigma \frac{r}{\sqrt{\Delta}} \sqrt{1 - \frac{(b^2 - a^2)}{r^2} + \frac{2M(b-a)^2}{r^3}} \\
& + \frac{B}{\sqrt{B^2 + C^2}} \frac{b}{\sqrt{\left( r^2 + a^2 + \frac{2Ma^2}{r} \right)}}. \tag{33}
\end{aligned}$$

The angle  $\alpha$  subtended by the direction along which the massless particle travels in the center-of-mass frame with respect to  $\hat{r}$  can be obtained from the velocity components (32), (33) by solving the equations below.

$$\sin \alpha = \frac{U_{cm}^{(\phi)}}{\sqrt{U_{cm}^{(r)2} + U_{cm}^{(\phi)2}}}; \quad \cos \alpha = \frac{U_{cm}^{(r)}}{\sqrt{U_{cm}^{(r)2} + U_{cm}^{(\phi)2}}} \tag{34}$$

We define the following critical angles for the radially ingoing particles with critical impact

parameters encountered earlier in Eqs. (28) and (30) :

$$\begin{aligned}
\alpha_1 &= \alpha(\sigma = -1, r, b = a) , \\
\alpha_2 &= \alpha(\sigma = -1, r, b = b_+(r)) , \\
\alpha_3 &= \alpha(\sigma = -1, r, b = b_-(r)) , \\
\alpha_4 &= \alpha(\sigma = -1, r, b = b_-(r_m)) .
\end{aligned} \tag{35}$$

Similarly, we define critical angles for radially outgoing particles with relevant critical impact parameters encountered in Eqs. (29) and (31) as follows:

$$\begin{aligned}
\alpha_5 &= \alpha(\sigma = +1, r, b = b_+(r)) , \\
\alpha_6 &= \alpha(\sigma = +1, r, b = b_-(r)) , \\
\alpha_7 &= \alpha(\sigma = +1, r, b = b_-(r_m)) .
\end{aligned} \tag{36}$$

We define

$$[[\alpha_i, \alpha_j]] = (\min(\alpha_i, \alpha_j), \max(\alpha_i, \alpha_j)) \tag{37}$$

If collision occurs at  $r < r_m$ , then the escape cone  $EC_{r < r_m}$  for the massless particles can be obtained from Eqs. (28), (29), (35) and (36). It is given by

$$EC_{r < r_m} = [[\alpha_1, \alpha_2]] \cup [[\alpha_5, \alpha_7]] , \tag{38}$$

whereas in the case collision occurs at  $r > r_m$  then the escape cone  $EC_{r > r_m}$  obtained from Eqs. (30), (31), (35) and (36) is given by

$$EC_{r > r_m} = [[\alpha_1, \alpha_2]] \cup [[\alpha_3, \alpha_4]] \cup [[\alpha_5, \alpha_6]] . \tag{39}$$

Thus, we have identified the escape cones within which the massless particle must be emitted in the center-of-mass frame so that it escapes to infinity.

### G. Collisional Penrose process

We now determine the conserved energy of the massless particle that is emitted within the escape cone. It depends on the direction along which the massless particle is emitted in the center-of-mass frame, i.e., it depends on the angle  $\alpha$  with  $\alpha \in EC_{r < r_m}$  if  $r < r_m$ , or  $\alpha$  with  $\alpha \in EC_{r > r_m}$

if  $r > r_m$ . Since the particle within the escape cone reaches infinity, the conserved energy of the particle is also its energy  $E$  measured by asymptotic observer.

From Eq. (21) it is given by the expression

$$E(\alpha) = \frac{m}{2} \frac{\sqrt{\Delta}A + \frac{2Ma}{r}C}{\sqrt{\left(r^2 + a^2 + \frac{2Ma^2}{r}\right)}} + \frac{m}{2} \frac{\sqrt{\Delta}\sqrt{B^2 + C^2} + \frac{2Ma}{r}\frac{AC}{\sqrt{B^2+C^2}}}{\sqrt{\left(r^2 + a^2 + \frac{2Ma^2}{r}\right)}} \cos \alpha \\ + \frac{m}{2} \frac{\frac{2Ma}{r}}{\sqrt{\left(r^2 + a^2 + \frac{2Ma^2}{r}\right)}} \frac{B}{\sqrt{B^2 + C^2}} \sqrt{A^2 - B^2 - C^2} \sin \alpha , \quad (40)$$

whereas the conserved energy of the other particle produced in the collision which is emitted in the opposite direction, denoted by  $E'$  can be obtained from Eq. (22) and is given by

$$E'(\alpha) = \frac{m}{2} \frac{\sqrt{\Delta}A + \frac{2Ma}{r}C}{\sqrt{\left(r^2 + a^2 + \frac{2Ma^2}{r}\right)}} - \frac{m}{2} \frac{\sqrt{\Delta}\sqrt{B^2 + C^2} + \frac{2Ma}{r}\frac{AC}{\sqrt{B^2+C^2}}}{\sqrt{\left(r^2 + a^2 + \frac{2Ma^2}{r}\right)}} \cos \alpha \\ - \frac{m}{2} \frac{\frac{2Ma}{r}}{\sqrt{\left(r^2 + a^2 + \frac{2Ma^2}{r}\right)}} \frac{B}{\sqrt{B^2 + C^2}} \sqrt{A^2 - B^2 - C^2} \sin \alpha . \quad (41)$$

Because of the phenomenon of frame-dragging, the timelike Killing vector  $k = \partial_t$  can become a spacelike vector and the conserved energy can take a negative value. For some set of directions  $\alpha$ , if  $E'(\alpha)$  turns out to be negative and then the energy of the particle escaping to infinity  $E(\alpha)$  would be larger than the combined energy of the colliding particles and collisional Penrose process would be at work. That is

$$E'(\alpha) < 0 \implies E(\alpha) > m(E_1 + E_2) . \quad (42)$$

The efficiency of the collisional Penrose process is defined as the ratio of the energy of the escaping particle created in the collision to the combined energy of the colliding particles.

$$\eta = \frac{E}{m(E_1 + E_2)} \quad (43)$$

It would be possible to generate ultra-high-energy particles, starting from the particles with moderate energies if the efficiency of the collisional Penrose process takes a value that is very large, i.e.,

$$\eta \gg 1 . \quad (44)$$

This condition is not met in the case of the Kerr black hole as it was demonstrated in [22],[23]. In this paper we show that efficiency of collisional Penrose process can be divergent for near-extremal overspinning Kerr geometry.

### H. Condition for the divergence of the efficiency of collisional Penrose process

We now identify the necessary conditions for the divergence of efficiency of the collisional Penrose process in the Kerr spacetime. First it is necessary for the conserved energy of the massless particle produced in the collision to diverge. Secondly this particle must be emitted within the escape cone so that it escapes to infinity.

The conserved energy of particle 3 is given by the expression as it can be read off from Eq. (21)

$$\begin{aligned}
E_3 = & \frac{m}{2} \frac{\sqrt{\Delta}A + \frac{2Ma}{r}C}{\sqrt{\left(r^2 + a^2 + \frac{2Ma^2}{r}\right)}} + \frac{m}{2} \frac{\sqrt{\Delta}\sqrt{B^2 + C^2} + \frac{2Ma}{r}\frac{AC}{\sqrt{B^2+C^2}}}{\sqrt{\left(r^2 + a^2 + \frac{2Ma^2}{r}\right)}} \cos \alpha \\
& + \frac{m}{2} \frac{\frac{2Ma}{r}}{\sqrt{\left(r^2 + a^2 + \frac{2Ma^2}{r}\right)}} \frac{B}{\sqrt{B^2 + C^2}} \sqrt{A^2 - B^2 - C^2} \sin \alpha ,
\end{aligned} \tag{45}$$

where  $A, B$  and  $C$  are given by Eq. (8) as follows:

$$\begin{aligned}
A = & \frac{1}{\sqrt{\Delta}} \frac{\left(E_1 \left(r^2 + a^2 + \frac{2Ma^2}{r}\right) - \frac{2Ma}{r}L_1\right)}{\sqrt{\left(r^2 + a^2 + \frac{2Ma^2}{r}\right)}} + \frac{1}{\sqrt{\Delta}} \frac{\left(E_2 \left(r^2 + a^2 + \frac{2Ma^2}{r}\right) - \frac{2Ma}{r}L_2\right)}{\sqrt{\left(r^2 + a^2 + \frac{2Ma^2}{r}\right)}} , \\
B = & \sigma_1 \frac{r}{\sqrt{\Delta}} \sqrt{E_1^2 - 1 + \frac{2M}{r} - \frac{L_1^2 - a^2(E_1^2 - 1)}{r^2} + \frac{2M(L_1 - aE_1)^2}{r^3}} \\
& + \sigma_2 \frac{r}{\sqrt{\Delta}} \sqrt{E_2^2 - 1 + \frac{2M}{r} - \frac{L_2^2 - a^2(E_2^2 - 1)}{r^2} + \frac{2M(L_2 - aE_2)^2}{r^3}} ,
\end{aligned}$$

and

$$C = \frac{L_1}{\sqrt{\left(r^2 + a^2 + \frac{2Ma^2}{r}\right)}} + \frac{L_2}{\sqrt{\left(r^2 + a^2 + \frac{2Ma^2}{r}\right)}} . \tag{46}$$

For the finite values of the radial coordinate  $r$  and geodesic parameters  $E_1, E_2, L_1$  and  $L_2$ , it is clear from Eq. (46) that  $C$  is always finite. Whereas,  $A$  and  $B$  can potentially diverge when  $\Delta \rightarrow 0$ , i.e.,

$$\begin{aligned}
C & = O(1) , \\
\Delta \rightarrow 0 & \implies A, B \sim \frac{1}{\sqrt{\Delta}} \rightarrow \infty .
\end{aligned} \tag{47}$$

Since  $A, B$  and  $C$  are the components of the net velocity of the two colliding particles which is timelike vector, we have  $A > 0$ ,  $A > |B|$  and  $A > |C|$ . Further, one can infer from Eq. (46) that  $B$  and  $C$  can never be zero together. Thus, when  $A$  is finite,  $E_3$  would be finite. For  $E_3$  to diverge,

$A$  must necessarily diverge. From Eq. (47),  $A$  diverges when  $\Delta \rightarrow 0$  and  $B$  can also potentially diverge. If both  $A$  and  $B$  diverge and are almost equal in magnitude, i.e., if  $(A - |B|)/A \rightarrow 0^+$ , then  $E_3$  is finite. For  $E_3$  to diverge  $A$  must be significantly larger than  $B$ , i.e.,  $(A - |B|)/A = O(1)$ . Thus, the requisite conditions for the divergence of  $E_3$  are as follows:

$$A \rightarrow \infty \quad \text{and} \quad \frac{A - |B|}{A} = O(1). \quad (48)$$

Interestingly, if the conditions stated above are met, then the center-of-mass energy of the two colliding particles also shows divergence. From Eq. (15), (47) and (48) these conditions above are equivalent to

$$E_{cm} = m\sqrt{A^2 - B^2 - C^2} \rightarrow \infty. \quad (49)$$

We obtain a crucial result here, namely, that we must have collision with the divergent center of mass energy if we want the efficiency of collisional Penrose process to diverge. Note that it is necessary but not a sufficient condition. The conserved energy of the massless particle created in the collision can diverge if the center-of-mass energy shows divergence. Further, the particle with large energy should also escape to infinity if the efficiency of collisional process is to show divergence.

It is possible to arrange for the collisions with the divergent center-of-mass energy around the near-extremal Kerr black holes and in the overspinning Kerr geometry [18],[41],[42]. However the efficiency of collisional Penrose process is finite in the case of black holes [22],[23], since the particles with large conserved energies produced in the ultra-high-energy collisions do not escape to infinity, but eventually enter the black hole. In this paper we show that in the overspinning Kerr geometry, particles with divergent conserved energies can also escape to infinity. Thus, the efficiency of collisional Penrose process shows divergence.

### I. Direction along which the colliding particles travel in center-of-mass frame

We determine the direction along which the colliding particles travel in the center-of-mass frame. This is needed for the calculation of the spectrum of the massless particles escaping to infinity, since the distribution of the emission of massless particles in the center-of-mass frame depends on the angle between the direction in which the colliding particles travel and direction along which the massless particles are emitted.

The colliding particles travel in  $\hat{r} - \hat{\phi}$  plane in the center-of-mass frame. The non-zero spatial components of velocity can be obtained from Eq. (12) by putting subscript  $i = 1, 2$  on relevant

quantities and are given by

$$\begin{aligned}
U_{i,cm}^{(r)} = & -\frac{\sqrt{B^2 + C^2}}{\sqrt{A^2 - B^2 - C^2}} \frac{1}{\sqrt{\Delta}} \frac{\left( \left( r^2 + a^2 + \frac{2Ma^2}{r} \right) E_i - \frac{2Ma}{r} L_i \right)}{\sqrt{\left( r^2 + a^2 + \frac{2Ma^2}{r} \right)}} \\
& + \frac{AC}{\sqrt{A^2 - B^2 - C^2} \sqrt{B^2 + C^2}} \frac{L_i}{\sqrt{\left( r^2 + a^2 + \frac{2Ma^2}{r} \right)}} \\
& + \frac{AB}{\sqrt{A^2 - B^2 - C^2} \sqrt{B^2 + C^2}} \sigma \frac{r}{\sqrt{\Delta}} \sqrt{E_i^2 - 1 + \frac{2M}{r} - \frac{L_i^2 - a^2 (E_i^2 - 1)}{r^2} + \frac{2M (L_i - aE_i)^2}{r^3}},
\end{aligned}$$

and

$$\begin{aligned}
U_{i,cm}^{(\phi)} = & -\frac{C}{\sqrt{B^2 + C^2}} \sigma \frac{r}{\sqrt{\Delta}} \sqrt{E_i^2 - 1 + \frac{2M}{r} - \frac{L_i^2 - a^2 (E_i^2 - 1)}{r^2} + \frac{2M (L_i - aE_i)^2}{r^3}} \\
& + \frac{B}{\sqrt{B^2 + C^2}} \frac{L_i}{\sqrt{\left( r^2 + a^2 + \frac{2Ma^2}{r} \right)}}.
\end{aligned} \tag{50}$$

The angle  $\alpha_{c,i}$  made by the direction along which the colliding particle travels in the center-of-mass frame can be obtained from the velocity components Eq. (50) by solving equations below

$$\sin \alpha_{c,i} = \frac{U_{i,cm}^{(\phi)}}{\sqrt{U_{i,cm}^{(r)2} + U_{i,cm}^{(\phi)2}}}; \quad \cos \alpha_{c,i} = \frac{U_{i,cm}^{(r)}}{\sqrt{U_{i,cm}^{(r)2} + U_{i,cm}^{(\phi)2}}}. \tag{51}$$

Since, from Eq. (14) in the center-of-mass frame, we have

$$U_{1,cm}^{(r)} + U_{2,cm}^{(r)} = U_{i,cm}^{(\phi)} + U_{i,cm}^{(\phi)} = 0. \tag{52}$$

From Eqs. (51) and (52), we obtain

$$\alpha_{c,2} = \pi + \alpha_{c,1} \tag{53}$$

i.e. two particles move in the opposite directions.

## J. Energy distribution of the massless particles escaping to infinity

We now compute the energy spectrum of the massless particles produced in the collisions escaping to infinity. We restrict ourselves to the collisions taking place at the specific radial coordinate since the ultra-high-energy collisions take place in a very narrow band over radial coordinate [18],[41],[42]. The energy of the massless particle produced in the collision depends on the conserved

energies and angular momenta of the colliding particles  $E_1, E_2, L_1$  and  $L_2$ , information whether particle is radially ingoing or outgoing, i.e., the values of  $\sigma_1$  and  $\sigma_2$ , and the angle  $\alpha$  at which the particle is emitted in the center-of-mass frame (40). A given value of energy  $E$  of the massless particle escaping to infinity can be achieved via different combinations of  $E_1, E_2, L_1, L_2, \sigma_1, \sigma_2$  and  $\alpha$ . We must count all configurations to determine the energy distribution function  $f[E]$ . That can be done in the following way:

$$f[E] \propto \sum_{\sigma_1, \sigma_2} \int d\alpha dE_1 dE_2 dL_1 dL_2 \bar{g}(E_1) \bar{g}(E_2) g(L_1) g(L_2) \times h(E_{cm}(E_1, E_2, L_1, L_2, \sigma_1, \sigma_2), \alpha - \bar{\alpha}) \delta(E - E_3(E_1, E_2, L_1, L_2, \sigma_1, \sigma_2, \alpha)) . \quad (54)$$

Here,  $\bar{g}(E_1)$ ,  $\bar{g}(E_2)$ ,  $g(L_1)$  and  $g(L_2)$  stand for the distribution of energies and angular momenta of the colliding particles.  $h(E_{cm}(E_1, E_2, L_1, L_2), \alpha - \bar{\alpha})$  is the angular distribution of the massless particles in the center of mass frame.  $\bar{\alpha}$  depicts the direction along which colliding particles travel (51) which can be determined from  $E_1, E_2, L_1$  and  $L_2$ . The angular distribution is dictated by the differential cross section of the underlying particle physics process. We assume that the angular distribution function  $h$  takes the following form:

$$h(E_{cm}, \gamma) = \sum_{n=0}^{\infty} h_n(E_{cm}) (\cos \gamma)^n . \quad (55)$$

Functions  $h_n(E_{cm})$  capture the information about the physics at the energy  $E_{cm}$ . To obtain the energy distribution  $f(E)$ , we integrate over all possible allowed values of conserved energies, angular momenta and angles subject to the constraint that their combination corresponds to the given energy  $E$  which is enforced by the Dirac's delta function. In the end we normalize  $f(E)$  over the entire range of the allowed energies.

### III. ULTRA-HIGH-ENERGY COLLISIONS IN THE OVERSPINNING KERR GEOMETRY

In this section we describe the process of ultra-high-energy collisions in the overspinning Kerr geometry. In the previous section we described the method we employ to study the collisional Penrose process in the Kerr spacetime. We now specialize to the overspinning Kerr spacetime geometry. We argued that for the divergence of the efficiency, it is necessary for particles to collide with divergent center-of-mass energy. We had identified the conditions under which it would be possible to have collisions with ultra-high-energy collisions in the overspinning Kerr geometry [41],[42]. We recapitulate the results here to orient ourselves to analyze the collisional Penrose process.

### A. General discussion

For the divergence of the center-of-mass energy of collision, it is necessary that  $A$  must diverge. For  $A$  to diverge,  $\Delta$  must take a value close to zero. From Eqs. (48) and (49),

$$E_{cm} = m\sqrt{A^2 - B^2 - C^2} \rightarrow \infty \implies A \rightarrow \infty \implies \Delta \rightarrow 0 . \quad (56)$$

For the overspinning Kerr geometry  $\Delta = (r^2 - 2Mr + a^2) = (r - M)^2 + (a^2 - M^2) > 0$  since  $a > M$ . The radial coordinate  $r = r_{min}$  at which  $\Delta$  is minimum and its minimum value  $\Delta_{min}$  are given by

$$r_{min} = M \quad ; \quad \Delta_{min} = a^2 - M^2 . \quad (57)$$

Thus, we consider the collision at the radial location  $r = r_{min} = M$  in the overspinning Kerr geometry with the spin parameter transcending the extremal value by an infinitesimal amount, i.e.

$$\begin{aligned} r_{collision} &= M , \\ a &= M(1 + \epsilon) \quad ; \quad \epsilon \rightarrow 0^+ . \end{aligned} \quad (58)$$

It is clear from Eq. (57) that the smaller the value of  $|B|$  is, the larger the center of mass energy of collision will be. For the fixed values of  $E_1, E_2, L_1$  and  $L_2$ ;  $|B|$  takes the smaller value if one of the particles is traveling in the radially inward direction and other particle is moving radially outwards, i.e.,  $\sigma_1\sigma_2 = -1$ , than the case where both the particles move in the radially inwards or radially outwards, i.e.,  $\sigma_1\sigma_2 = +1$ . From Eqs. (8) and (57), we can infer that

$$\begin{aligned} |B(E_1, E_2, L_1, L_2, \sigma_1\sigma_2 = -1)| &< |B(E_1, E_2, L_1, L_2, \sigma_1\sigma_2 = 1)| \\ \implies E_{cm}(E_1, E_2, L_1, L_2, \sigma_1\sigma_2 = -1) &> E_{cm}(E_1, E_2, L_1, L_2, \sigma_1\sigma_2 = 1) . \end{aligned} \quad (59)$$

Therefore, we would like to consider the case where one of the particles travels in the radially outward direction and other particle travels in the radially inward direction. Without the loss of generality we assume that the particle 1 moves in the radially outward direction.

$$\sigma_1 = +1 \quad ; \quad \sigma_2 = -1 \quad (60)$$

We also assume that both the particles start from rest at infinity. In other words, particles are non-relativistic when they are faraway from the singularity, which is a reasonable assumption. When particles fall towards singularity, they attain relativistic velocities in the high-curvature region. From Eq. (2), we can set the conserved energies of two particles to unity, i.e.,

$$E_1 = E_2 = 1 . \quad (61)$$

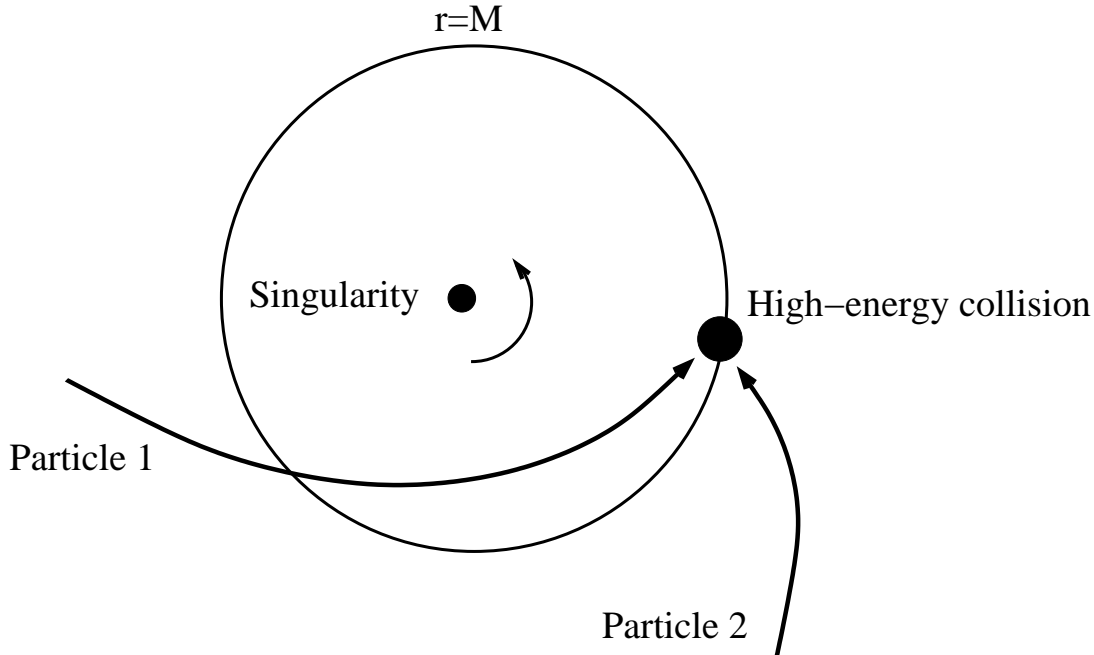


FIG. 3: High-energy collision at  $r = M$  around the Kerr naked singularity. Particle 1 is an initially ingoing particle which turns back inside the circle  $r = M$  and reappears at  $r = M$  as an outgoing particle. Particle 2 is an ingoing particle at  $r = M$ . The center-of-mass energy of collision shows divergence when the Kerr spin parameter transcends the extremal value by a small amount i.e.  $a = M(1 + \epsilon)$  ;  $\epsilon \rightarrow 0^+$ .

### B. Allowed range for the angular momenta of the two particles

Particle 1 starting from infinity which is initially infalling must turn back at  $r < M$  so as to appear at  $r = M$  as an outgoing particle. Whereas particle 2 should appear at  $r = M$  as an ingoing particle. For this to happen the angular momenta of the two particles must be in the appropriate range.

Turning points for the particle with conserved energy  $E = 1$  and angular momentum per unit mass  $L$  can be obtained from Eq. (2) by solving

$$\frac{2M}{r} - \frac{L^2}{r^2} + \frac{2M}{r^3}(L - a)^2 = 0 \quad (62)$$

and are given by

$$r = r_{\pm} = \frac{L^2}{4M} \left( 1 \pm \sqrt{1 - \frac{16M^2(L - a)^2}{L^4}} \right). \quad (63)$$

The outer turning point  $r = r_+$  is relevant for our discussion since we are interested in the particles which fall towards the singularity from infinity. The turning points (63) exist for the angular

momenta in the following range:

$$L < L_- = -2M \left( \sqrt{1 + \frac{a}{M}} + 1 \right), \quad 2M \left( \sqrt{1 + \frac{a}{M}} - 1 \right) = L_+ < L. \quad (64)$$

As we increase the angular momentum above  $L_+$ , i.e., for  $L > L_+$  or decrease it below  $L_-$ , i.e., for  $L < L_-$ , the outer turning point  $r_+$  shifts radially outwards. The minimum values of the radial coordinates of the turning point,  $r_{++}$  and  $r_{+-}$ , for the positive and negative angular momenta, from Eqs. (63) and (64) are given by

$$r_{++} = M \left( \sqrt{1 + \frac{a}{M}} - 1 \right)^2 \quad \text{and} \quad r_{+-} = M \left( \sqrt{1 + \frac{a}{M}} + 1 \right)^2, \quad (65)$$

respectively. Note that  $r_{+-}$  is always above the collision point, whereas  $r_{++}$  is below the collision point for sufficiently small values of the spin parameter. That is,

$$M < a < 3M \implies r_{++} < M \quad \text{and} \quad r_{+-} > M. \quad (66)$$

Since we are interested in the spin parameter which is slightly above the extremality,  $r_{++}$  is below the collision point. The angular momentum required for the particle to turn back at  $r = M$  obtained from Eq. (62) is given by

$$L_{+,m} = 2a - \sqrt{2a^2 - 2M^2}. \quad (67)$$

Particle 1 must admit a turning point at the radial coordinate  $r < M$  so that it appears at  $r = M$  as an outgoing particle starting from infinity as an ingoing particle. It must turn back between  $r = r_{++}$  and  $r = M$ . Thus, from Eqs. (64), (65) and (67), its angular momentum  $L_1$  must be in the following range:

$$2M \left( \sqrt{1 + \frac{a}{M}} - 1 \right) < L_1 < \left( 2a - \sqrt{2a^2 - 2M^2} \right). \quad (68)$$

Particle 2 appears at  $r = M$  as an ingoing particle starting from infinity. Thus, it should not admit a turning point at  $r > M$ . Thus, from Eqs. (64), (65) and (67), its angular momentum  $L_2$  must satisfy the condition

$$-2M \left( 1 + \sqrt{1 + \frac{a}{M}} \right) < L_2 < \left( 2a - \sqrt{2a^2 - 2M^2} \right). \quad (69)$$

Thus, we obtained the conditions that must be imposed on the angular momenta of the two colliding particles so that we have a collision in the desired setting. The angular momentum of particle 1 must take a positive value, while the angular momentum of particle 2 can take a positive as well as negative value.

### C. Center-of-mass energy of collision

We now compute the center-of-mass energy of collision. The collision takes place at the radial coordinate  $r = M$  and is between particle 1 that is radially outgoing and particle 2 that is radially ingoing.

We calculate  $A$ ,  $B$  and  $C$  to the leading order. From Eqs. (8), (58), (60), (61), (68) and (69), we obtain

$$A = \frac{(4M - (L_1 + L_2))}{\sqrt{2\epsilon M}}, B = \frac{(L_2 - L_1)}{\sqrt{2\epsilon M}}, C = \frac{(L_1 + L_2)}{2M}. \quad (70)$$

The center-of-mass energy of collision to the leading order obtained from Eqs. (56) and (70) is given by

$$E_{cm} = m\sqrt{A^2 - B^2 - C^2} = \sqrt{\frac{2}{\epsilon}} \frac{m}{M} \sqrt{(2M - L_1)(2M - L_2)}. \quad (71)$$

In the near-extremal limit, as  $\epsilon \rightarrow 0$ , the center-of-mass energy shows divergence

$$\lim_{\epsilon \rightarrow 0^+} E_{cm} \rightarrow \infty. \quad (72)$$

### D. Sign of B and C

We now determine the sign of  $B$  and  $C$ . The sign of  $B$  which is the radial component of net velocity of the two colliding particles, depending on whether it is positive, negative or zero, determines whether the center of mass moves in the radially outward direction, radially inward direction or does not move in the radial direction.

From Eqs. (8), (58), (60) and (61) we obtain

$$B = \frac{1}{\sqrt{a^2 - M^2}} \left( \sqrt{2M^2 - L_1^2 + 2(L_1 - a)^2} - \sqrt{2M^2 - L_2^2 + 2(L_2 - a)^2} \right). \quad (73)$$

It is clear from Eq. (73) that depending on whether  $\bar{B}$  is greater than, less than or equal to zero, we can have  $B$  positive, negative or zero, respectively, where

$$\bar{B} = \left( -L_1^2 + 2(L_1 - a)^2 \right) - \left( -L_2^2 + 2(L_2 - a)^2 \right) = (L_2 - L_1)(4a - (L_1 + L_2)). \quad (74)$$

From Eqs. (68) and (69) we know that  $(4a - (L_1 + L_2)) > +2\sqrt{2a^2 - 2M^2} > 0$ . Therefore, the sign of  $\bar{B}$  and thus of  $B$  is determined by  $(L_2 - L_1)$ .

From Eqs. (8), (57) and (61), we obtain

$$C = \frac{(L_1 + L_2)}{\sqrt{M^2 + 3a^2}} \quad (75)$$

Thus, the sign of  $C$  is determined by  $(L_1 + L_2)$ .

We tabulate the different cases below. The values of  $L_1$  and  $L_2$  are assumed to be in their allowed range given by Eqs. (68) and (69).

$B$ and $C$	$L_1$ and $L_2$
$B > 0$ and $C > 0$	$L_2 > L_1$
$B = 0$ and $C > 0$	$L_2 = L_1$
$B < 0$ and $C > 0$	$L_2 < L_1$ and $L_2 > -L_1$
$B < 0$ and $C = 0$	$L_2 < L_1$ and $L_2 = -L_1$
$B < 0$ and $C < 0$	$L_2 < L_1$ and $L_2 < -L_1$

TABLE I: Sign of  $B$  and  $C$ . We tabulate the sign of  $B$  and  $C$ , depending on the values of  $L_1$  and  $L_2$  in the allowed range.

While analyzing the collisional Penrose process, we must deal with the cases  $B > 0$ ,  $B < 0$  and  $B = 0$ , separately. In case of the overspinning Kerr geometry, the results as we show would be qualitatively the same irrespective of the sign of  $B$ , which is not the case for Kerr black holes [28].

#### IV. COLLISIONAL PENROSE PROCESS IN THE OVERSPINNING KERR GEOMETRY

In the previous section we described the process of ultra-high-energy collisions in the overspinning Kerr geometry which is the pre-requisite to the efficient energy extraction. In this section we analyze the collisional Penrose process and show that its efficiency shows divergence. We assume that two massless particles are produced in the collision. We obtain the escape cones for the massless particle to reach to infinity and energy of the particle within the escape cone.

The collision point which is at  $r = M$  is within  $r = r_m \sim 4M$  as it can be shown from Eqs. (27) and (58). Thus, the escape cones for the massless particles are given by Eq. (38), i.e.,

$$EC = [[\beta_1, \beta_2]] \cup [[\beta_3, \beta_4]] , \quad (76)$$

where the critical angles appearing in the expression above are given by

$$\begin{aligned} \beta_1 &= \alpha_1 = \alpha(\sigma = -1, b = a) , \\ \beta_2 &= \alpha_2 = \alpha\left(\sigma = -1, b = 2a - \sqrt{a^2 - M^2}\right) , \\ \beta_3 &= \alpha_5 = \alpha\left(\sigma = +1, b = 2a - \sqrt{a^2 - M^2}\right) , \end{aligned}$$

$$\beta_4 = \alpha_7 = \alpha \left( \sigma = +1, b = a - \frac{\left( M^{\frac{2}{3}} + \left( a + \sqrt{a^2 - M^2} \right)^{\frac{2}{3}} \right)^3}{\left( a + \sqrt{a^2 - M^2} \right)} \right). \quad (77)$$

### A. Center of mass moves radially outwards: $B > 0$

We now analyze the collisional Penrose process in the case where the center of mass moves in the radially outward direction, i.e.,  $B > 0$ . From Table I, it happens when  $L_2 > L_1$  and consequently we also have  $C > 0$ . The behavior of  $A$ ,  $B$  and  $C$  deduced from Eqs. (8), (58), (60) and (61) is as depicted below

$$A = O\left(\epsilon^{-\frac{1}{2}}\right), \quad B = O\left(\epsilon^{-\frac{1}{2}}\right), \quad C = O\left(\epsilon^0\right). \quad (78)$$

The first colliding particle which is an outgoing particle at  $r = M$  moves along the direction which makes angle  $\alpha_{c,1}$ , which can be obtained from Eqs. (51), (58), (60) and (61), is given by

$$\alpha_{c,1} = -\sqrt{\frac{\epsilon}{2}} \left[ \left( \frac{L_1}{L_2 - L_1} \right) \sqrt{\frac{2M - L_2}{2M - L_1}} + \left( \frac{L_2}{L_2 - L_1} \right) \sqrt{\frac{2M - L_1}{2M - L_2}} \right]. \quad (79)$$

In the near-extremal limit, as  $\epsilon \rightarrow 0^+$ , we have  $\alpha_{c,1} \rightarrow 0$ . Thus, the particle moves almost along  $+\hat{r}$  direction in the center-of-mass frame. Whereas, the second colliding particle moves almost along  $-\hat{r}$  direction.

We now calculate the critical angles  $\beta_1$ ,  $\beta_2$ ,  $\beta_3$  and  $\beta_4$  from Eqs. (34), (58), (60), (61) and (77), which is given by:

$$\begin{aligned} \beta_1 &= \pi - \sqrt{2\epsilon} \frac{L_2}{(L_2 - L_1)} \sqrt{\frac{2M - L_2}{2M - L_1}}, \\ \beta_2 &= \beta_3 = \pi - \arcsin \left( \frac{2\sqrt{2M - L_2}\sqrt{2M - L_1}}{(4M - L_1 - L_2)} \right), \\ \beta_4 &= -\frac{\sqrt{2\epsilon}}{9} \sqrt{\frac{2M - L_1}{2M - L_2}} \frac{(L_1 + 8L_2)}{(L_2 - L_1)}. \end{aligned} \quad (80)$$

In the near-extremal limit  $\epsilon \rightarrow 0^+$ , the limit values of the critical angles are given by  $\beta_1 \rightarrow \pi$  and  $\beta_4 \rightarrow 0$ .  $\beta_2 = \beta_3$  since  $r = M$  is a turning point for  $b = 2a - \sqrt{a^2 - M^2}$  as we had shown earlier in Eq. (67). A radially outgoing massless particle generated in the collision will escape to infinity if it is emitted along the angle which lies in the range  $\alpha \in [[\beta_3, \beta_4]]$  and radially ingoing massless particle escapes to infinity if it is emitted along the angle  $\alpha \in [[\beta_1, \beta_2]]$ . The escape fraction, i.e., the probability for the massless particle to escape to infinity assuming the isotropic distribution

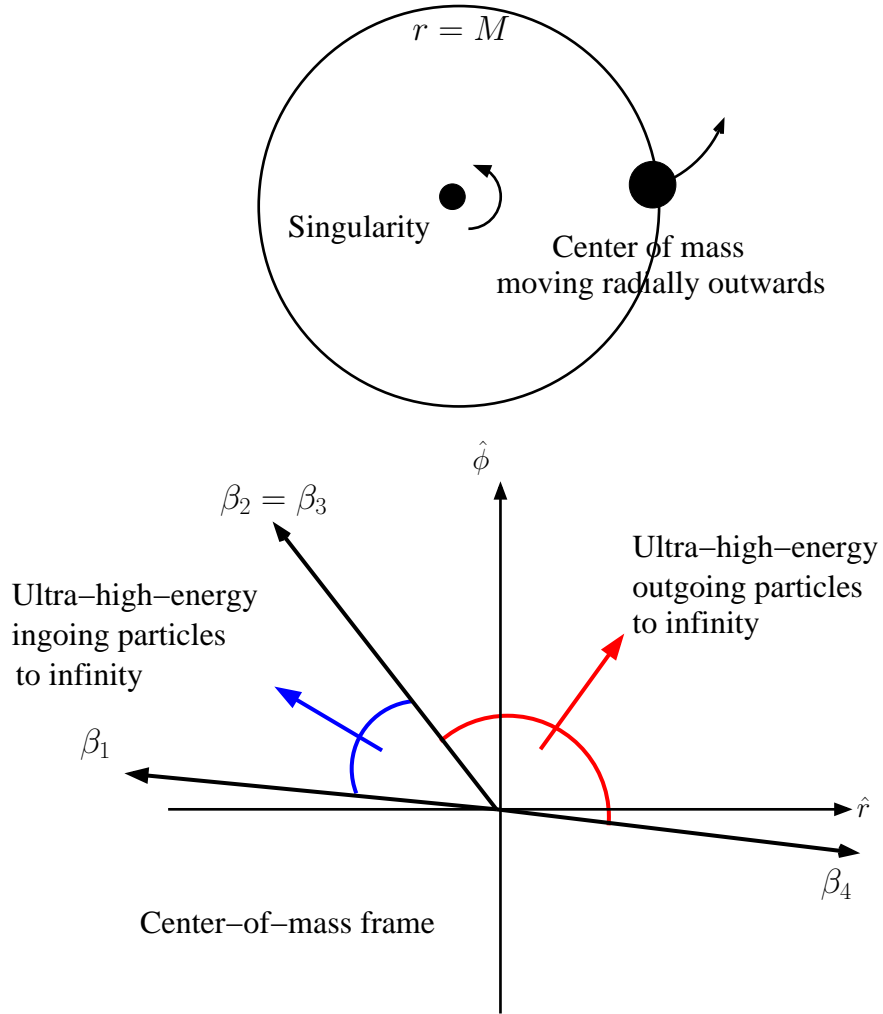


FIG. 4: In the case  $B > 0$ , the center of mass moves in the radially outward direction. Massless particles that are emitted in the angular range  $[[\beta_1, \beta_2]]$  move radially inwards, encounter a turning point and then escape to infinity. They are depicted by the blue arrow. Massless particles emitted in the angular range  $[[\beta_3, \beta_4]]$  are emitted in the radially outward direction and escape to infinity. They are depicted by the red arrow. Particles reach infinity with ultra-high-energy unless  $\alpha$  is close to 0 or  $\pi$ .

for the emission in the center-of-mass frame is given by the ratio of the angular range of escape cones to the entire angular range. We can find

$$E.F. = \frac{|\beta_1 - \beta_2| + |\beta_3 - \beta_4|}{2\pi} \rightarrow \frac{1}{2}, \quad (81)$$

in the limit  $\epsilon \rightarrow 0^+$ . Therefore, in the near-extremal limit, the escape fraction is half. Thus, if we consider a large number of collisions, then half of the particles produced in the collisions will escape to infinity.

The energy of the massless particle as measured by an observer at infinity is obtained from

Eqs. (40), (58), (60) and (61). Unless the particle is emitted along the angle which is very close to 0 or  $\pi$ , to the leading order it is given by

$$E(\alpha) = \frac{m}{\sqrt{2M}} \frac{\sqrt{2M - L_2} \sqrt{2M - L_1}}{\sqrt{\epsilon}} \sin \alpha . \quad (82)$$

The energy shows divergence in the near-extremal limit, i.e.,

$$\lim_{\epsilon \rightarrow 0^+} E \rightarrow \infty . \quad (83)$$

The energy of the other particle which is produced in the collision and moves in the opposite direction is given by

$$E'(\alpha) = -\frac{m}{\sqrt{2M}} \frac{\sqrt{2M - L_2} \sqrt{2M - L_1}}{\sqrt{\epsilon}} \sin \alpha . \quad (84)$$

It takes a large negative value, i.e.,

$$\lim_{\epsilon \rightarrow 0^+} E' \rightarrow -\infty . \quad (85)$$

Thus, the collisional Penrose process is at work and is responsible for ultra-high-energy particle escaping to infinity.

If the massless particle emitted along the angle which is sufficiently close to 0 or  $\pi$ , the energy turns out to be finite. For instance for the massless particle traveling along the angles  $\beta_1$  and  $\beta_4$ , their energies obtained from Eqs. (40), (58), (60) and (61) are given by

$$E(\beta_1) = \frac{m}{M} (2M - L_2) \quad (86)$$

and

$$E(\beta_4) = \frac{1}{9} \frac{m}{M} (2M - L_1) , \quad (87)$$

respectively.

However the proportion of the particles which escape to infinity with finite energy is minuscule. Almost all the particles that escape to infinity are ultra-high-energy particles with divergent energies.

### B. Center of mass does not move in the radial direction: $B = 0$

Here we consider the case where the center of mass does not move in the radial direction, i.e.,  $B = 0$ . From Table I, it happens when  $L_2 = L_1 = L$  and we have  $C > 0$ . The behavior of  $A$ ,  $B$  and  $C$  can be deduced from Eqs. (8), (58), (60) and (61) and is given by

$$A = O\left(\epsilon^{-\frac{1}{2}}\right) , \quad B = 0 , \quad C = O(\epsilon^0) . \quad (88)$$

The first colliding particle moves along the direction which makes angle  $\alpha_{c,1}$ , which can be obtained from Eqs. (51), (58), (60) and (61), is given by

$$\alpha_{c,1} = -\frac{\pi}{2} . \quad (89)$$

First particle moves almost along  $-\hat{\phi}$  direction in the center-of-mass frame. The second colliding particle moves almost along  $+\hat{\phi}$  direction.

We now calculate the critical angles  $\beta_1, \beta_2, \beta_3$  and  $\beta_4$  from Eqs. (34), (58), (60), (61) and (77) as follows:

$$\begin{aligned} \beta_1 &= \frac{\pi}{2} - \frac{\sqrt{2\epsilon}M}{2M-L} , \\ \beta_2 &= \beta_3 = 0 , \\ \beta_4 &= -\frac{\pi}{2} - \frac{\sqrt{2\epsilon}(7M+L)}{9(2M-L)} , \end{aligned} \quad (90)$$

as  $\epsilon \rightarrow 0^+$ . The limit values of the critical angles in the near-extremal limit are given by  $\beta_1 \rightarrow \frac{\pi}{2}$  and  $\beta_4 \rightarrow -\frac{\pi}{2}$ . Again  $\beta_2 = \beta_3$  since  $r = M$  is a turning point for  $b = 2a - \sqrt{a^2 - M^2}$  as we had shown earlier in Eq. (67). A radially outgoing massless particle generated in the collision will escape to infinity if it is emitted along an angle which lies in the range  $\alpha \in [[\beta_3, \beta_4]]$  and a radially ingoing massless particle escapes to infinity if it is emitted along an angle  $\alpha \in [[\beta_1, \beta_2]]$ .

The escape fraction assuming the isotropic distribution for the emission in the center-of-mass frame is given by

$$E.F. = \frac{|\beta_1 - \beta_2| + |\beta_3 - \beta_4|}{2\pi} \rightarrow \frac{1}{2} , \quad (91)$$

in the limit  $\epsilon \rightarrow 0^+$ . Therefore, in the near-extremal limit, the escape fraction is half.

The energy of the massless particle as measured by an observer at infinity is obtained from Eqs. (40), (58), (60) and (61). For the particles emitted along the angles not very close to 0 or  $\pi$ , energy to the leading order is given by

$$E(\alpha) = \frac{m}{\sqrt{2M}} \frac{\sqrt{2M-L_2}\sqrt{2M-L_1}}{\sqrt{\epsilon}} \cos \alpha . \quad (92)$$

Thus, the energy shows divergence in the near-extremal limit, i.e.,

$$\lim_{\epsilon \rightarrow 0^+} E \rightarrow \infty . \quad (93)$$

The energy of the other particle moving in the opposite direction is given by

$$E'(\alpha) = -\frac{m}{\sqrt{2M}} \frac{\sqrt{2M-L_2}\sqrt{2M-L_1}}{\sqrt{\epsilon}} \cos \alpha . \quad (94)$$

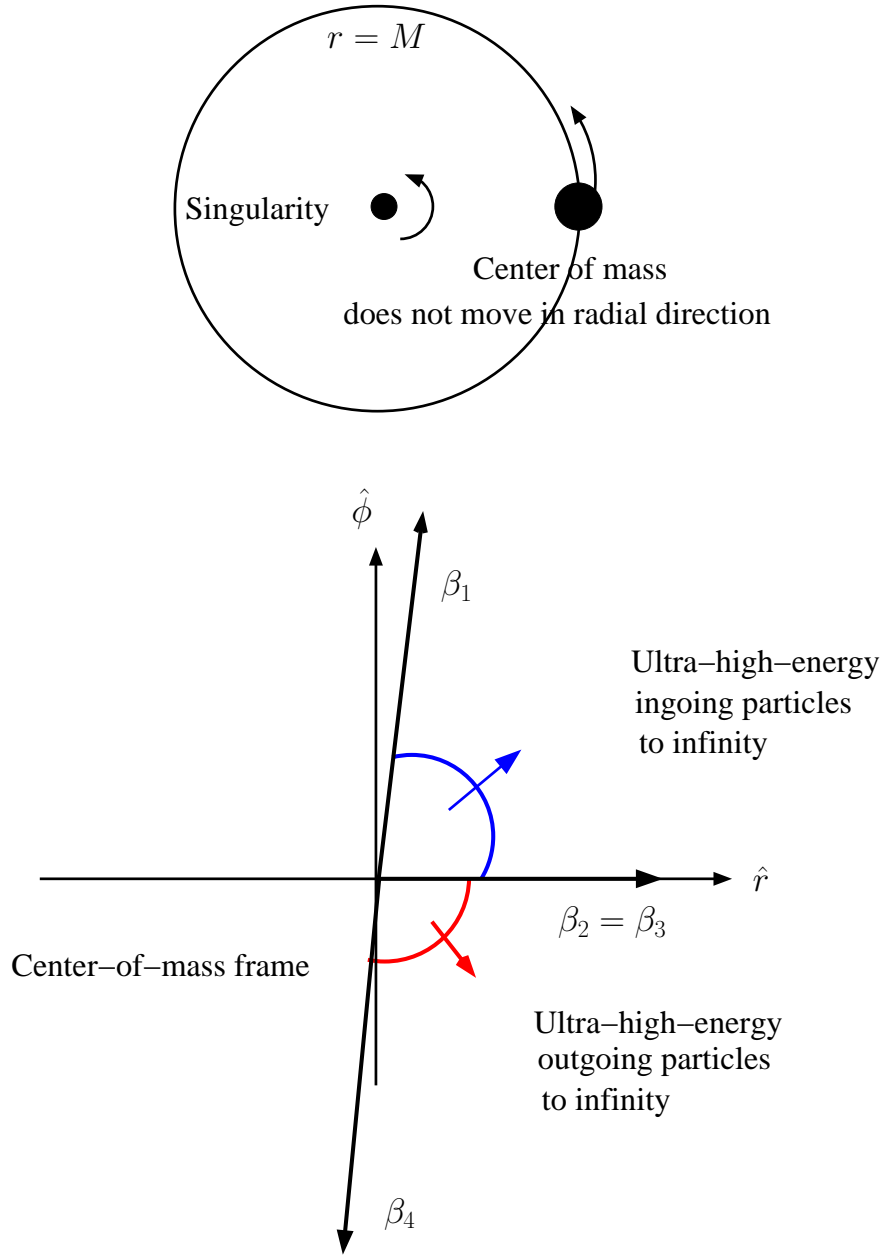


FIG. 5: In the case  $B = 0$ , the center of mass does not move in the radial direction. Massless particles that are emitted in the angular range  $[[\beta_1, \beta_2]]$  move radially inwards, encounter a turning point and then escape to infinity. They are depicted by the blue arrow. Massless particles emitted in the angular range  $[[\beta_3, \beta_4]]$  are emitted in the radially outward direction and escape to infinity. They are depicted by the red arrow. Particles reach infinity with ultra-high-energy unless  $\alpha$  is close to  $-\pi/2$  or  $\pi/2$ .

It tends to negative infinity, i.e.,

$$\lim_{\epsilon \rightarrow 0^+} E' \rightarrow -\infty. \quad (95)$$

This confirms the fact that the collisional Penrose process is at work and is responsible for the generation of ultra-high-energy particle escaping to infinity.

If the massless particle emitted along the angle which is sufficiently close to 0 or  $\pi$ , the energy turns out to be finite. For instance for the massless particle traveling along angles  $\beta_1$  and  $\beta_4$ , the energies obtained from Eqs. (40), (58), (60) and (61) are given by

$$E(\beta_1) = \frac{m}{M}(2M - L) , \quad (96)$$

and

$$E(\beta_4) = \frac{1}{9} \frac{m}{M}(2M - L) , \quad (97)$$

respectively.

The proportion of the particles which escape to infinity with finite energy is minuscule. Almost all the particles that escape to infinity are ultra-high-energy particles.

### C. Center of mass moves radially inwards: $B < 0$

We now consider the case where the center of mass moves in the direction radially inwards, i.e.,  $B < 0$ . From Table I, it happens when  $L_2 < L_1$  and we can have  $C$  either positive, negative or zero. The behavior of  $A$ ,  $B$  and  $C$ , as inferred from Eqs. (8), (58), (60) and (61), is given by

$$A = O(\epsilon^{-\frac{1}{2}}) , B = O(\epsilon^{-\frac{1}{2}}) , C = O(\epsilon^0) . \quad (98)$$

The angle  $\alpha_{c,1}$ , along which the first colliding particle moves, can be obtained from Eqs. (51), (58), (60) and (61), and is given by

$$\alpha_{c,1} = \pi + \sqrt{\frac{\epsilon}{2}} \left( \left( \frac{L_1}{L_1 - L_2} \right) \sqrt{\frac{2M - L_2}{2M - L_1}} + \left( \frac{L_2}{L_1 - L_2} \right) \sqrt{\frac{2M - L_1}{2M - L_2}} \right) , \quad (99)$$

in the limit  $\epsilon \rightarrow 0^+$ . The first particle moves almost along  $-\hat{r}$  direction, whereas the second colliding particle moves almost along  $+\hat{r}$  direction in the center-of-mass frame.

We now calculate the critical angles  $\beta_1$ ,  $\beta_2$ ,  $\beta_3$  and  $\beta_4$  from Eqs. (34), (58), (60), (61) and (77)

as follows:

$$\begin{aligned}
\beta_1 &= \sqrt{2\epsilon} \frac{L_2}{(L_1 - L_2)} \sqrt{\frac{2M - L_2}{2M - L_1}}, \\
\beta_2 &= \beta_3 = -\pi + \arcsin \left( \frac{2\sqrt{2M - L_2}\sqrt{2M - L_1}}{(4M - L_1 - L_2)} \right), \\
\beta_4 &= -\pi + \frac{\sqrt{2\epsilon}}{9} \sqrt{\frac{2M - L_1}{2M - L_2}} \frac{(L_1 + 8L_2)}{(L_1 - L_2)}.
\end{aligned} \tag{100}$$

The limit values of critical angles in the near-extremal limit  $\epsilon \rightarrow 0^+$  are given by  $\beta_1 \rightarrow 0$  and  $\beta_4 \rightarrow -\pi$ . We have  $\beta_2 = \beta_3$  from Eq. (67). The massless particle produced in the collision will escape to infinity if it is emitted along an angle which lies in the range  $\alpha \in [[\beta_3, \beta_4]]$  and the radially ingoing massless particle escapes to infinity if it is emitted along angle  $\alpha \in [[\beta_1, \beta_2]]$ . The escape fraction if we assume isotropic distribution for the emission of massless particles in the center-of-mass frame is given by

$$E.F. = \frac{|\beta_1 - \beta_2| + |\beta_3 - \beta_4|}{2\pi} \rightarrow \frac{1}{2}. \tag{101}$$

In the near-extremal limit, the escape fraction is again half.

The energy of the massless particle as measured by observer at infinity is obtained from Eqs. (40), (58), (60) and (61). Unless the angle  $\alpha$  is very close to 0 or  $\pi$ , its energy to the leading order is given by

$$E(\alpha) = -\frac{m}{\sqrt{2M}} \frac{\sqrt{2M - L_2}\sqrt{2M - L_1}}{\sqrt{\epsilon}} \sin \alpha. \tag{102}$$

Their energy shows divergence in the near-extremal limit

$$\lim_{\epsilon \rightarrow 0^+} E \rightarrow \infty. \tag{103}$$

The energy of the second particle moving in the opposite direction is given by

$$E'(\alpha) = +\frac{m}{\sqrt{2M}} \frac{\sqrt{2M - L_2}\sqrt{2M - L_1}}{\sqrt{\epsilon}} \sin \alpha. \tag{104}$$

It tends to negative infinity, i.e.,

$$\lim_{\epsilon \rightarrow 0^+} E' \rightarrow -\infty. \tag{105}$$

Thus, the collisional Penrose process is at work and accounts for the the generation of ultra-high-energy particle escaping to infinity.

If the massless particle emitted along the angle which is sufficiently close to 0 or  $\pi$ , its energy would be finite. For instance, for the massless particle traveling along angles  $\beta_1$  and  $\beta_4$ , their

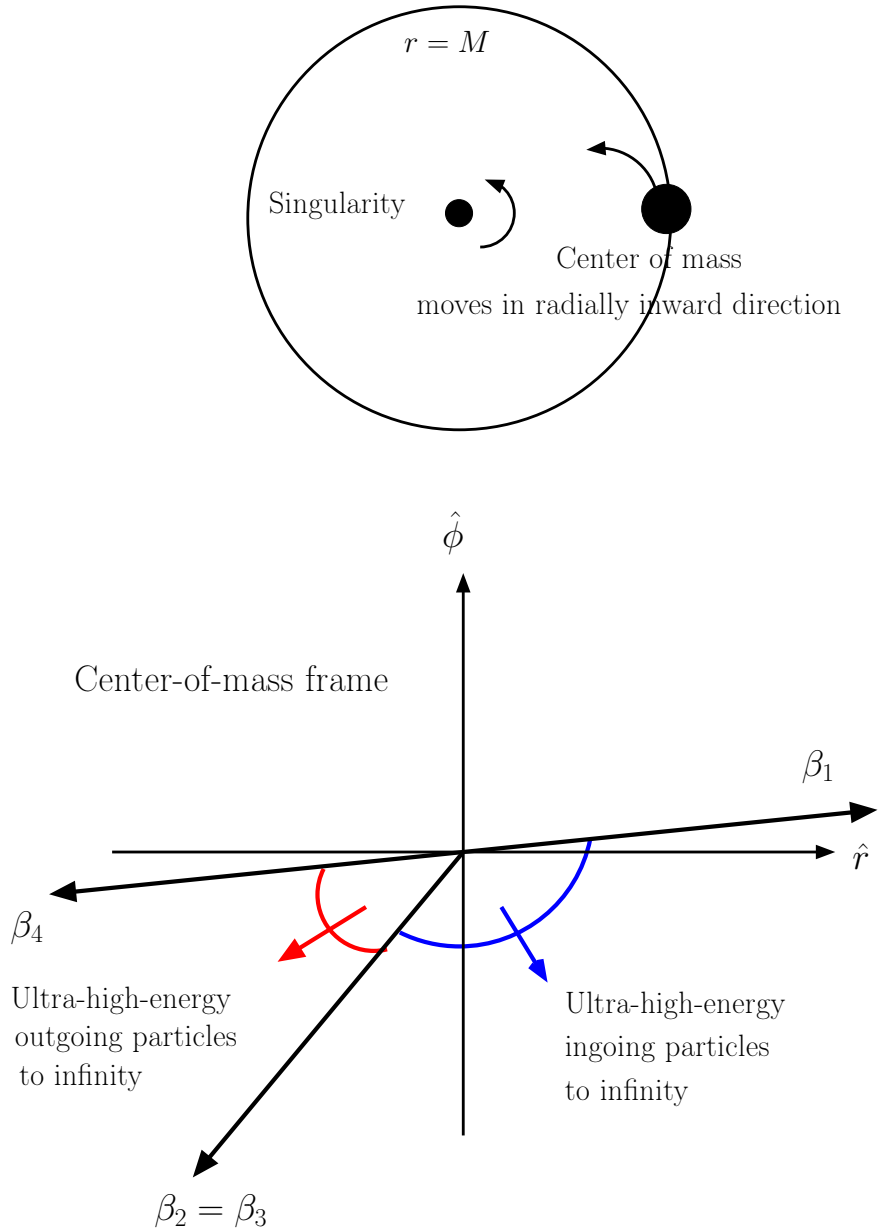


FIG. 6: In the case  $B < 0$ , the center of mass moves in the radially inward direction. Massless particles that are emitted in the angular range  $[[\beta_1, \beta_2]]$  move radially inwards, encounter a turning point and escape to infinity. They are depicted by the blue arrow. Massless particles emitted in the angular range  $[[\beta_3, \beta_4]]$  are emitted in the radially outward direction and escape to infinity. They are depicted by the red arrow. Particles reach infinity with ultra-high-energy unless  $\alpha$  is close to 0 or  $\pi$ .

energies obtained from Eqs. (40), (58), (60) and (61) are given by

$$E(\beta_1) = \frac{m}{M} (2M - L_2) , \quad (106)$$

and

$$E(\beta_4) = \frac{1}{9} \frac{m}{M} (2M - L_1) , \quad (107)$$

respectively.

The proportion of the particles which escape to infinity with finite energy is minuscule. Almost all the particles that escape to infinity are ultra-high-energy particles.

#### D. Divergence of efficiency of collisional Penrose process

We now compute the efficiency of the collisional Penrose process. For further analysis, we find it convenient to rotate the coordinate axes by the angle  $\pi/2$  in the case where  $B = 0$  and by the angle  $\pi$  in the case  $B < 0$ . From Eqs. (82), (92) and (102), the energy of the particle that escapes to infinity can now be written as

$$E = \frac{m}{\sqrt{2M}} \frac{\sqrt{2M - L_2} \sqrt{2M - L_1}}{\sqrt{\epsilon}} \sin \alpha . \quad (108)$$

The efficiency of the collisional Penrose process which is defined by the ratio of conserved energy of the particle escaping to infinity to the total conserved energy of the colliding particles is given by

$$\eta = \frac{E}{2m} = \frac{1}{2\sqrt{2M}} \frac{\sqrt{2M - L_2} \sqrt{2M - L_1}}{\sqrt{\epsilon}} \sin \alpha . \quad (109)$$

For a fixed value of the parameter  $\epsilon$  depicting the deviation of Kerr geometry from extremality, the efficiency of collisional Penrose process is maximum when  $\alpha = \frac{\pi}{2}$ , i.e., the particle is emitted along the direction orthogonal to the direction in which the colliding particles travel and angular momenta  $L_1$  and  $L_2$  take minimum possible values in the allowed range (68) and (69), namely  $L_1 = 2M \left( \sqrt{1 + \frac{a}{M}} - 1 \right)$  and  $L_2 = -2M \left( \sqrt{1 + \frac{a}{M}} + 1 \right)$ . From Eq. (109), it is given by

$$\eta_{max} = \frac{1}{\sqrt{\epsilon}} . \quad (110)$$

The maximum efficiency goes to infinity in the near-extremal limit where the spin parameter transcends the extremal value by an infinitesimally small number, i.e.,

$$\lim_{\epsilon \rightarrow 0^+} \eta_{max} \rightarrow \infty . \quad (111)$$

Thus, we have demonstrated that the efficiency of collisional Penrose process can be arbitrarily large in the overspinning Kerr spacetime geometry. This implies that it will be possible to extract large energy and generate ultra-high-energy particles starting with the particles with moderate energies. In the next section, we explore the implications of the super-efficient collisional Penrose process from the point of view of astrophysics as well as fundamental particle physics.

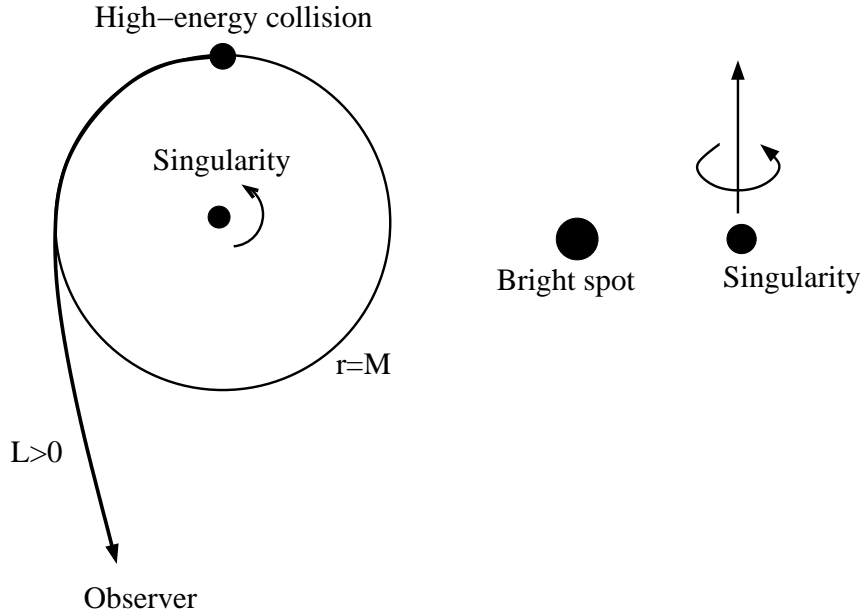


FIG. 7: Bright spot. Left Panel: Ultra-high-energy particles created in the high-energy collision have a positive angular momentum. Thus, they co-rotate with the singularity. Right Panel: High-energy particles seem to originate from the bright spot on that side of the singularity which is rotating towards the observer.

## V. BRIGHT SPOT OF ULTRA-HIGH-ENERGY PARTICLES

The angular momentum of the massless particles escaping to infinity obtained from Eqs. (23), (58), (60) and (61) given by the following expression to the leading order:

$$L = \sqrt{2}m \frac{\sqrt{2M - L_2} \sqrt{2M - L_1}}{\sqrt{\epsilon}} \sin \alpha . \quad (112)$$

This expression is valid for all the three cases  $B > 0$ ,  $B = 0$  and  $B < 0$  after rotating the coordinate axes by the angles  $\pi/2$  and  $\pi$  in the last two cases. Here  $\alpha$  is assumed to be away from 0 and  $\pi$  and thus it corresponds to the massless particles with ultra-high-energies. Note that the angular momentum is always positive for the particles that are emitted with large energies. Particles with positive angular momentum travel in the same way in which the naked singularity rotates. Thus, to the distant observer, they seem to emerge from that side of the singularity, which is rotating towards the observer. Further, the impact parameter of all ultra-high-energy particles, obtained from Eqs. (108) and (112) is given by the approximate constant value given below:

$$b = \frac{L}{E} = 2M . \quad (113)$$

Thus, ultra-high-energy particles seem to emerge from a bright spot of a narrow width.

We now compute the angular location of the bright spot relative to the singularity as observed by a distant observer in LNRF at the large value of the radial coordinate  $r$ . The results would not change much for the non-corotating observers since the frame-dragging is minuscule at large radii. Consider a radially outgoing massless particle with impact parameter  $b$ . The spatial components of velocity in LNRF can be read off from Eq. (7)

$$\begin{aligned} U_{LNRF}^{(\phi)}(b, r) &= \frac{b}{\sqrt{\left(r^2 + a^2 + \frac{2Ma^2}{r}\right)}}, \\ U_{LNRF}^{(r)}(b, r) &= \frac{r}{\sqrt{\Delta}} \sqrt{1 - \frac{(b^2 - a^2)}{r^2} + \frac{2M(b-a)^2}{r^3}}, \\ U_{LNRF}^{(\theta)}(b, r) &= 0. \end{aligned} \quad (114)$$

The three-velocity of the massless particle obtained from Eq. (114) is given by

$$V_{LNRF}^{(i)}(b, r) = \frac{U_{LNRF}^{(i)}(b, r)}{\sqrt{\delta_{jk} U_{LNRF}^{(j)}(b, r) U_{LNRF}^{(k)}(b, r)}}. \quad (115)$$

The direction in which the particle travels as seen by LNRF observer is dictated by its three-velocity. Since all the ultra-high-energy massless particles produced in high-energy collisions around the naked singularity have the impact parameter  $b = 2M$ , the direction in which they travel is dictated by  $V_{LNRF}^{(i)}(2M, r)$ . Consider a hypothetical massless particle with the zero impact parameter  $b = 0$  which emerges from the singularity and reaches the distant observer. The trajectory of this particle is bent due to the frame-dragging in the Kerr spacetime. The direction in which it travels with respect to the observer is dictated by  $V_{LNRF}^{(i)}(0, r)$ . The angular location of the bright spot from where high-energy particles appear to emerge from relative to the singularity can be obtained by computing the angle between  $V_{LNRF}^{(i)}(2M, r)$  and  $V_{LNRF}^{(i)}(0, r)$ . It is given by

$$\sin \xi = \sqrt{1 - \left(\delta_{jk} V_{LNRF}^{(j)}(2M, r) V_{LNRF}^{(k)}(0, r)\right)^2}. \quad (116)$$

From Eqs. (114), (115) and (116), we obtain

$$\sin \xi = \frac{U_{LNRF}^{(\phi)}(2M, r)}{\sqrt{U_{LNRF}^{(\phi)2}(2M, r) + U_{LNRF}^{(r)2}(2M, r)}}. \quad (117)$$

Thus, in the large  $r$  limit, the expression for the angle  $\xi$  obtained from Eqs. (114) and (117) is given by

$$\xi = \frac{2M}{r}. \quad (118)$$

This is the angular location of the bright spot on that side of the singularity, which is rotating towards us from where high-energy particles appear to originate to the distant observer.

## VI. DISTRIBUTION OF ENERGY OF MASSLESS PARTICLES

We now compute the energy distribution of the ultra-high-energy massless particles escaping to infinity. As described earlier, we focus only on the collisions that occur at  $r = M$  and compute their contribution to the spectrum. The collisions are between ingoing and outgoing particles, i.e.,  $\sigma_1 = +1$  and  $\sigma_2 = -1$ . The conserved energies of the colliding particles are taken to be unity  $E_1 = E_2 = 1$ . This allows us to omit summation over  $\sigma_1$  and  $\sigma_2$  and also the integration over  $E_1$  and  $E_2$  in Eq. (54). Thus, from Eqs. (54), (71) and (108), we obtain the following expression for the spectrum of the massless particles:

$$f[E] \propto \int d\alpha dL_1 dL_2 g(L_1) g(L_2) h\left(\sqrt{\frac{2}{\epsilon}} \frac{m}{M} \sqrt{(2M - L_1)(2M - L_2)}, \alpha\right) \times \delta\left(E - \frac{m}{\sqrt{2}M} \frac{\sqrt{2M - L_2} \sqrt{2M - L_1}}{\sqrt{\epsilon}} \sin \alpha\right). \quad (119)$$

We need to integrate over all possible values of angular momenta  $L_1$  and  $L_2$  and angles of emission  $\alpha$  of massless particles in the center-of-mass frame.

We integrate over angle  $\alpha$  using the following property of Dirac's delta function:

$$\delta(f(x)) = \sum_i \frac{\delta(x - x_i)}{|f'(x_i)|}, \text{ where } f(x_i) = 0. \quad (120)$$

From Eqs. (119) and (120),

$$f[E] \propto \int d\alpha dL_1 dL_2 g(L_1) g(L_2) \frac{\left(h\left(\sqrt{\frac{2}{\epsilon}} \frac{m}{M} \sqrt{(2M - L_1)(2M - L_2)}, \beta\right) + h\left(\sqrt{\frac{2}{\epsilon}} \frac{m}{M} \sqrt{(2M - L_1)(2M - L_2)}, \pi - \beta\right)\right)}{\sqrt{\left(\frac{m}{\sqrt{2}M} \frac{\sqrt{2M - L_2} \sqrt{2M - L_1}}{\sqrt{\epsilon}}\right)^2 - E^2}} \quad (121)$$

where  $\beta$  is an angle such that

$$\sin \beta = \frac{2E}{\sqrt{\frac{2}{\epsilon}} \frac{m}{M} \sqrt{(2M - L_1)(2M - L_2)}}. \quad (122)$$

We now use the expansion of angular distribution function  $h$  we proposed earlier in Eq. (55). For the analysis carried out in this paper we retain only first two relevant terms. We obtain

$$f[E] \propto \int dL_1 dL_2 g(L_1) g(L_2) \frac{h_0}{\sqrt{y(2M - L_1)(2M - L_2) - E^2}} + \int dL_1 dL_2 g(L_1) g(L_2) \frac{h_2 \sqrt{y(2M - L_1)(2M - L_2) - E^2}}{(y(2M - L_1)(2M - L_2))}, \quad (123)$$

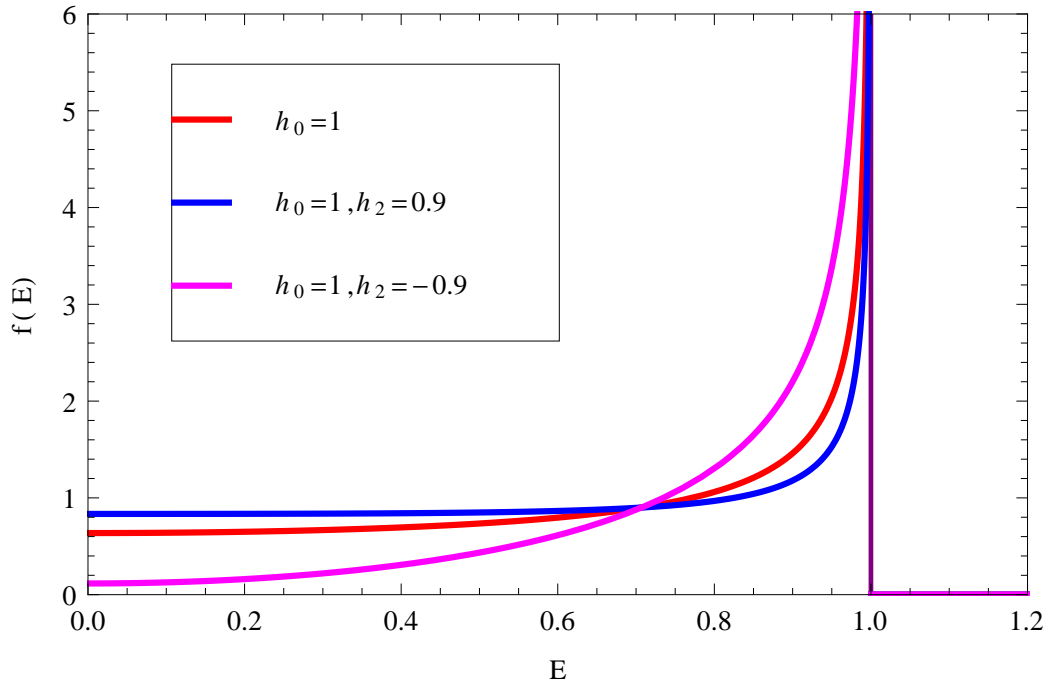


FIG. 8: Energy distribution function  $f[E]$  is plotted here, where  $E$  is expressed in units of  $E_m$ . We assume that the angular momenta of both the colliding particles take the fixed values. The distribution function shows divergence at  $E = E_m$ . The plots are made for three different cases A.  $h_0 = 1, h_2 = 0$ , B.  $h_0 = 1, h_2 = 0.9$ , and C.  $h_0 = 1, h_2 = -0.9$ .

where  $y = m^2/(2M^2\epsilon)$ . The first term in the expression above corresponds to the contribution from the isotropic emission, whereas the second term corresponds to the leading order contribution from anisotropic emission in the center-of-mass frame. We also assume that neither  $h_0$  nor  $h_2$  varies significantly at higher energies and both can be taken as constant. This assumption allows us to analytically calculate the spectrum. In a more realistic calculation, the variation of  $h_0$  and  $h_2$  must be taken into account.  $h_0$  and  $h_2$  can be calculated from the differential cross section of underlying particle physics process.

We now compute the energy distribution function by making different assumptions regarding the distribution of angular momenta.

#### A. Both $L_1$ and $L_2$ are fixed

We first make a naive assumption that the angular momentum of particle 1 takes a fixed value  $L_1^*$  and that of particle 2 takes a fixed value  $L_2^*$  in the allowed range, i.e., the distribution of the

angular momenta is Dirac's delta function

$$g(L_1) = \delta(L_1 - L_1^*) ; g(L_2) = \delta(L_2 - L_2^*) . \quad (124)$$

From Eq. (124), we can integrate over  $L_1$  and  $L_2$ . The energy distribution function, which is given by Eq. (123), can now be written as

$$f[E] \propto \left( \frac{h_0}{\sqrt{y(2M - L_1^*)(2M - L_2^*) - E^2}} + \frac{h_2 \sqrt{y(2M - L_1^*)(2M - L_2^*) - E^2}}{(y(2M - L_1^*)(2M - L_2^*))} \right) . \quad (125)$$

It is clear from the expression above that the highest allowed value of the energy  $E$  is

$$E_m = \sqrt{y(2M - L_1^*)(2M - L_2^*)} . \quad (126)$$

Thus, the spectrum admits an upper cut-off at energy  $E_m$  which can go to infinity in the near-extremal limit. We normalize the distribution function (125) so that

$$\int_0^{E_m} dE f(E) = 1 . \quad (127)$$

From Eqs. (125) and (127), we obtain a normalized distribution function as

$$f[E] = \frac{2}{\pi \left( h_0 + \frac{h_2}{2} \right)} \left( \frac{h_0}{\sqrt{E_m^2 - E^2}} + \frac{h_2 \sqrt{E_m^2 - E^2}}{E_m^2} \right) . \quad (128)$$

We plot  $f[E]$  in Fig. 8. Quite remarkably, the distribution function shows divergence at  $E = E_m$ . This is an artifact of the choice of Dirac's delta distribution for both the angular momenta and disappears when we relax this assumption as we will show later.

### B. $L_1$ is fixed and $L_2$ follows uniform distribution

Relaxing the assumption that angular momenta of both the particles are fixed, we now assume that the angular momentum of particle 1 is  $L_1^*$ , a fixed value in the allowed range, while the angular momentum  $L_2$  follows uniform distribution over the entire allowed range.

$$g(L_1) = \delta(L_1 - L_1^*) ; g(L_2) = C \quad (129)$$

Integrating over  $L_1$  using Dirac's delta function, Eq. (119) can be written as

$$f[E] \propto \int_{L_2^l}^{L_2^u} dL_2 \left( \frac{h_0}{\sqrt{y(2M - L_1^*)(2M - L_2) - E^2}} + \frac{h_2 \sqrt{y(2M - L_1^*)(2M - L_2) - E^2}}{(y(2M - L_1^*)(2M - L_2))} \right) , \quad (130)$$

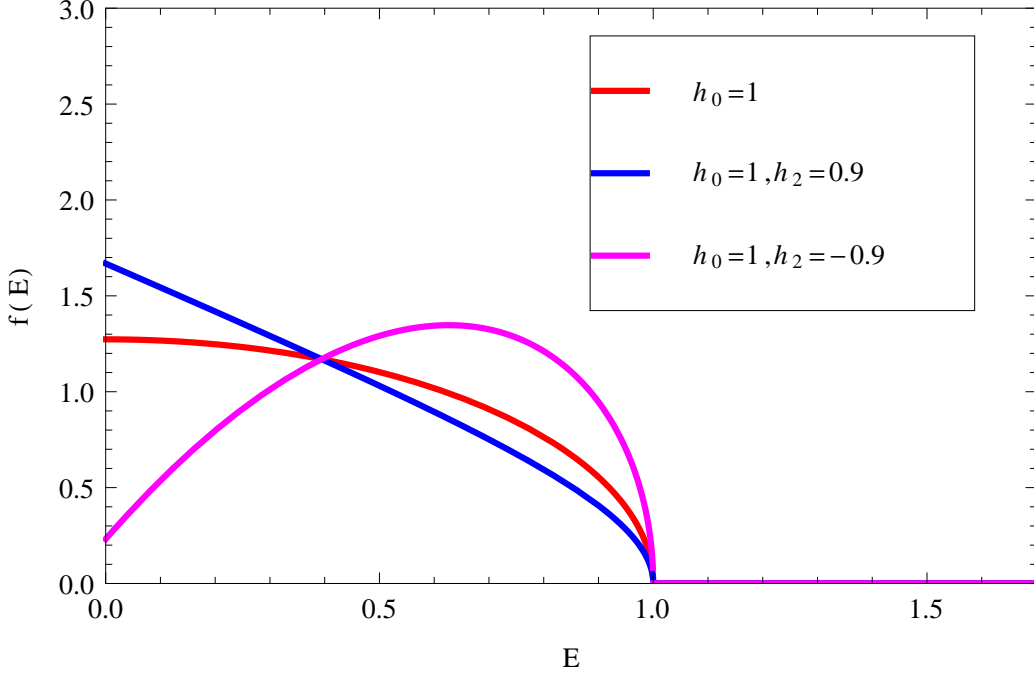


FIG. 9: Energy distribution function  $f[E]$  is plotted, where  $E$  is expressed in units of  $E_m$ . The angular momentum of one of the particles is fixed while the angular momentum of the other particle follows uniform distribution over the entire allowed range. The distribution function sharply declines and goes to zero at  $E = E_m$ . The plots are made for three different cases: A.  $h_0 = 1, h_2 = 0$ , B.  $h_0 = 1, h_2 = 0.9$ , and C.  $h_0 = 1, h_2 = -0.9$ .

where  $L_2^l$  is the lowest value of the angular momentum stated in Eq. (69) and  $L_2^u$  is given by

$$L_2^u = 2M - \frac{E^2}{y(2M - L_1^*)}. \quad (131)$$

Integrating over  $L_2$ , the distribution function Eq. (130) can be written as

$$f[E] \propto (h_0 + h_2) \sqrt{y(2M - L_1^*)(2M - L_2^l) - E^2} - h_2 E \arctan \frac{\sqrt{y(2M - L_1^*)(2M - L_2^l) - E^2}}{E}. \quad (132)$$

It is clear from the expression above that the highest allowed value of the energy  $E$  is

$$E_m = \sqrt{y(2M - L_1^*)(2M - L_2^l)}. \quad (133)$$

The energy spectrum admits an upper bound  $E_m$ , which can go to infinity in the near-extremal limit. The normalized distribution function can be written as

$$f[E] = \frac{4}{\pi \left(h_0 + \frac{h_2}{2}\right)} \frac{1}{E_m^2} \left( (h_0 + h_2) \sqrt{E_m^2 - E^2} - h_2 E \arctan \frac{\sqrt{E_m^2 - E^2}}{E} \right). \quad (134)$$

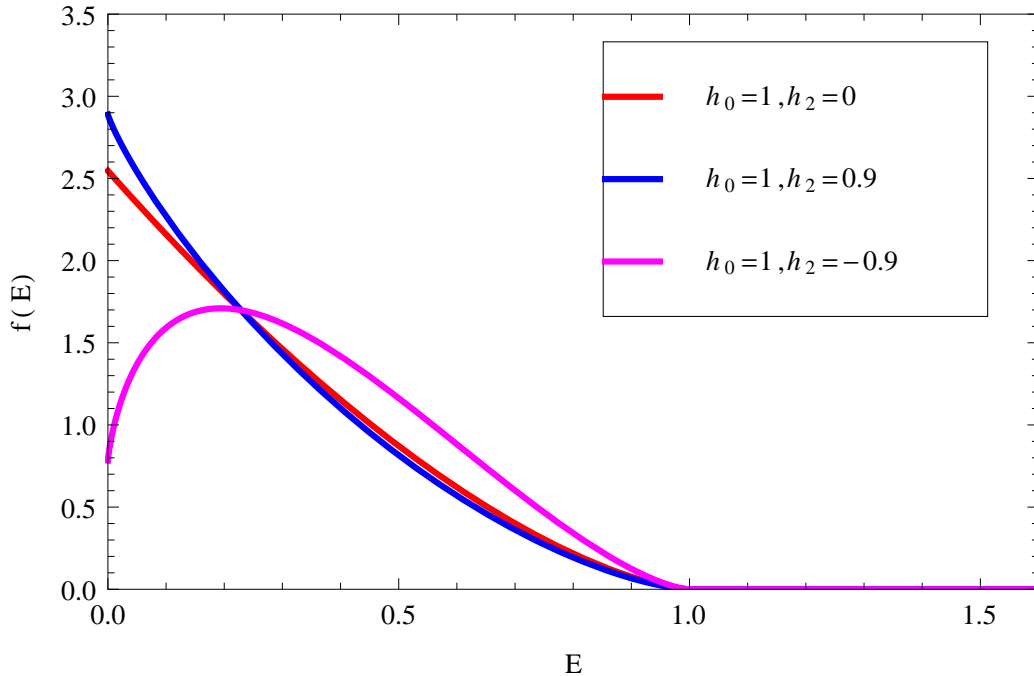


FIG. 10: Energy distribution function  $f[E]$  is plotted here, where  $E$  is expressed in units of  $E_m$ . The angular momenta of both the particles follow uniform distribution over the entire allowed range, which is a physically realistic assumption. The distribution function goes to zero at  $E = E_m$  rather slowly and smoothly. Plots are made for three different cases: A.  $h_0 = 1, h_2 = 0$ , B.  $h_0 = 1, h_2 = 0.9$ , and C.  $h_0 = 1, h_2 = -0.9$ . The distribution is drastically different, depending on whether  $h_2$  is positive or negative.

The energy distribution function goes to zero very sharply when the energy approaches highest energy  $E = E_m$ . The divergence of the distribution when both the angular momenta were fixed disappears even when one of them is allowed to vary over different values. The behavior is qualitatively different for positive and negative values of the parameter  $h_2$  which depicts the anisotropic emission of the massless particles in the center-of-mass frame.

### C. Both $L_1$ and $L_2$ follow uniform distribution

We now make the assumption that the angular momenta of both the particles are uniformly distributed over the entire allowed range. This is a quite realistic assumption. That is,

$$g(L_1) = C_1 \text{ and } g(L_2) = C_2 . \quad (135)$$

In this case both the integrals over  $L_1$  and  $L_2$  are non-trivial.

$$f[E] \propto \int_{L_1^l}^{L_1^u} dL_1 \int_{L_2^l}^{L_2^u(L_1)} dL_2 \left( \frac{h_0}{\sqrt{y(2M-L_1)(2M-L_2)-E^2}} + \frac{h_2 \sqrt{y(2M-L_1)(2M-L_2)-E^2}}{(y(2M-L_1)(2M-L_2))} \right) \quad (136)$$

The lower limits of integration  $L_1^l$  and  $L_2^l$  are the lowest permissible values of the angular momenta discussed in Eqs. (68) and (69). While  $L_1^u$  and  $L_2^u(L_1)$  are given by

$$L_1^u = 2M - \frac{E^2}{y(2M-L_2^l)} \text{ and } L_2^u(L_1) = 2M - \frac{E^2}{y(2M-L_1)}, \quad (137)$$

respectively. Integrating over  $L_1$  and  $L_2$ , we can write the distribution function (136) as

$$\begin{aligned} f[E] \propto & 2(h_0 + h_2) \left( \sqrt{y(2M-L_1^l)(2M-L_2^l)-E^2} - E \arctan \frac{\sqrt{y(2M-L_1^l)(2M-L_2^l)-E^2}}{E} \right) \\ & - i h_2 E \left( \frac{\pi^2}{24} + \frac{1}{2} \left( \arctan \frac{\sqrt{y(2M-L_1^l)(2M-L_2^l)-E^2}}{E} \right)^2 \right) \\ & + h_2 E \arctan \frac{\sqrt{y(2M-L_1^l)(2M-L_2^l)-E^2}}{E} \log \left( 1 + e^{2i \arctan \frac{\sqrt{y(2M-L_1^l)(2M-L_2^l)-E^2}}{E}} \right) \\ & - i h_2 E \frac{1}{2} \text{PolyLog} \left( 2, -e^{2i \arctan \frac{\sqrt{y(2M-L_1^l)(2M-L_2^l)-E^2}}{E}} \right). \end{aligned} \quad (138)$$

The upper limit on the allowed value of the energy  $E$  is

$$E_m = \sqrt{y(2M-L_1^l)(2M-L_2^l)}. \quad (139)$$

Thus, we obtain an upper cut-off  $E_m$ , which can go to infinity in the near-extremal limit.

The normalized distribution can be written as

$$f(E) = \frac{4}{\pi(h_0 + \frac{3}{4}h_2)} \frac{1}{E_m^2} \left( 2(h_0 + h_2) \left( \sqrt{E_m^2 - E^2} - E \arctan \frac{\sqrt{E_m^2 - E^2}}{E} \right) - h_2 E \Sigma(E) \right), \quad (140)$$

where

$$\begin{aligned} \Sigma(E) = & i \frac{\pi^2}{24} + i \frac{1}{2} \left( \arctan \frac{\sqrt{E_m^2 - E^2}}{E} \right)^2 - \arctan \frac{\sqrt{E_m^2 - E^2}}{E} \log \left( 1 + e^{2i \arctan \frac{\sqrt{E_m^2 - E^2}}{E}} \right) \\ & + i \frac{1}{2} \text{PolyLog} \left( 2, -e^{2i \arctan \frac{\sqrt{E_m^2 - E^2}}{E}} \right). \end{aligned} \quad (141)$$

The distribution function goes to zero rather slowly and smoothly as the highest energy  $E = E_m$  is reached as compared to the previous case, where one of the angular momentum followed Dirac's

delta distribution. The distribution is concave for non-negative values of  $h_2$ . For negative values of  $h_2$  it becomes concave as energy approaches  $E = E_m$ . The distribution was always convex when one of the angular momentum was fixed. The behavior is quite different in the two cases, where  $h_2$  is positive and negative. This implies that the anisotropy in the emission of the massless particles which is dictated by the differential cross section of the underlying particle physics process is imprinted on the spectrum in a subtle way. Thus, the observation of the spectrum of ultra-high-energy particles can allow us distinguish different particle physics models at ultra-high energies where particles collide.

In all three cases, the energy distribution function depends only on  $E_m$ ,  $h_0$  and  $h_1$ . As mentioned earlier  $h_0$  and  $h_1$  are dictated by the fundamental physics.  $E_m$  which is the upper bound on the energy of the massless particle, is dictated by the mass of the colliding particle  $m$  and the parameter  $\epsilon$  depicting the deviation of the Kerr spin parameter from extremal value. From (126), (133) and (139),  $E_m$  turns out to be  $O(\frac{m}{\sqrt{\epsilon}})$ . We rewrite it as

$$\frac{m}{\sqrt{\epsilon}} = \left( \frac{m}{m_p} \right) \frac{1}{\sqrt{\epsilon}} \text{GeV} \quad (142)$$

where  $m_p$  is the mass of proton. For  $E_m$  to be comparable to the astrophysically relevant values  $\epsilon$  must be very small. For  $E_m$  to correspond to the maximum energy of the ultra-high energy cosmic rays  $10^{11}$  GeV and that of ultra-high energy neutrinos  $10^6$  GeV, we must have  $\epsilon = 10^{-22}$  and  $\epsilon = 10^{-12}$  respectively, if we assume that the massless particles are produced in the collision of proton-like particles. As we explain in the next section, the over-spinning Kerr geometry is driven towards the extremality as a consequence of the collisional Penrose process. Thus such small values of the parameter  $\epsilon$  can be realized quite naturally.

## VII. UPPER BOUND ON THE ENERGY

The expressions for the conserved energy and angular momentum of the massless particle produced in the collision, from (108) and (112), are given by

$$E = \frac{m}{\sqrt{2M}} \frac{\sqrt{2M - L_2} \sqrt{2M - L_1}}{\sqrt{\epsilon}} \sin \alpha, \quad (143)$$

and

$$L = \sqrt{2} m \frac{\sqrt{2M - L_2} \sqrt{2M - L_1}}{\sqrt{\epsilon}} \sin \alpha, \quad (144)$$

respectively. If the massless particle is emitted in the upper plane in the center of mass frame away from  $\hat{r}$  axis, i.e. when  $\alpha \in (0, \pi)$ , its conserved energy as well as conserved angular momentum is

extremely large. Whereas for the massless particle which is emitted in the diametrically opposite direction with respect to the first particle in the lower plane for which  $\alpha \in (\pi, 2\pi)$ , both conserved energy as well as the angular momentum takes a value which is large and negative.

Particle emitted in the upper plane away from  $\hat{r}$  axis escapes and carries large energy and angular momentum to infinity. Whereas the particle emitted in the lower plane with large negative energy and angular momentum eventually hits the singularity, thereby reducing the Kerr mass and angular momentum parameters.

The conserved energy  $E$  and angular momentum  $L$  of the massless particle escaping to infinity are related by

$$L = 2ME . \quad (145)$$

Thus final Kerr mass parameter  $M_f$  and spin parameter  $a_f$  are given by

$$M_f = M - E \quad \text{and} \quad a_f = \frac{Ma - L}{M - E} . \quad (146)$$

It is clear from the expression above that the final spin parameter is smaller than its initial value, i.e.,  $a_f < a$ . Hence the collisional Penrose process leads to the reduction of the Kerr spin parameter and the over-spinning Kerr geometry is driven towards the extremality when the back-reaction is taken into account. Thus the rotational energy is being extracted from the over-spinning Kerr spacetime as in the case of Kerr black hole.

The present calculation is meaningful so long as the final configuration is over-spinning Kerr geometry. The final dimensionless spin parameter can be obtained from (146) and is given by

$$\frac{a_f}{M_f} = \frac{1 - \frac{2E}{M} + \epsilon}{1 - \frac{2E}{M} + \frac{E^2}{M^2}} , \quad (147)$$

where we have used the relation  $a = M(a + \epsilon)$ . It must be larger than unity. Thus we get

$$\epsilon > \frac{E^2}{M^2} . \quad (148)$$

Eliminating  $\epsilon$  from (143) and (148), we get an upper bound on the energy of the massless particle as

$$E < \left(1 - \frac{L_1}{2M}\right)^{\frac{1}{4}} \left(1 - \frac{L_2}{2M}\right)^{\frac{1}{4}} \sqrt{2 \sin \alpha} \times \sqrt{mM} . \quad (149)$$

Thus the energy of the massless particle produced is at most  $O(\sqrt{mM})$ . We rewrite  $\sqrt{mM}$  as

$$\sqrt{mM} = 3.2 \times 10^{28} \left(\frac{m}{m_p}\right)^{\frac{1}{2}} \left(\frac{M}{M_\odot}\right)^{\frac{1}{2}} \text{ GeV} , \quad (150)$$

where  $m_p$  and  $M_\odot$  are the masses of proton and sun respectively. As we stated earlier, the energy of ultra-high energy cosmic rays is upto  $10^{11}$  GeV and that of the ultra-high energy neutrinos is upto  $10^6$  GeV. Thus the upper bound is still so high that it can be of great interest from astrophysical and particle physics point of view.

### VIII. CONCLUSION

In this paper we presented a novel mechanism to generate the ultra-high-energy particles starting with particles with the moderate energies that is exclusively based on gravity exploiting the collisional Penrose process. All other acceleration mechanisms proposed so far make use of electromagnetic interaction to accelerate particles to high energy. We consider an overspinning Kerr geometry transcending the extremality by an infinitesimal amount  $a = M(1 + \epsilon)$ , where we take the limit  $\epsilon \rightarrow 0^+$ . Overspinning spacetime geometries occur quite naturally in the context of string theory and also may appear as a transient configuration in the process of gravitational collapse of regular matter cloud. We showed that the ultra-high-energy collisions are necessary to produce the particles with large energies in the Kerr spacetime. Collisions with divergent center-of-mass energy can occur around the near-extremal Kerr black holes as well as in the overspinning Kerr spacetime geometry. In this paper we demonstrate that the efficiency of the collisional Penrose process can diverge in the overspinning Kerr geometry in near-extremal limit  $\eta \sim 1/\sqrt{\epsilon} \rightarrow \infty$ , while the efficiency is always finite in the context of the Kerr black holes.

We consider two identical massive particles that start from rest at infinity and fall towards the singularity. One of the particles turns back at  $r < M$  as it encounters the angular momentum barrier and appears at  $r = M$  as an outgoing particle. The other particle appears at  $r = M$  as an ingoing particle where it collides with an outgoing particle. The center-of-mass energy of collision shows divergence in the near-extremal limit. We considered a process where the two colliding particles are scattered to produce two massless particles. All the particles were assumed to move on the equatorial plane, for simplicity, since it allows to carry out a fully analytical analysis of the collisional Penrose process. We made a transition to the center-of-mass tetrad since the differential cross section of the underlying particle physics process is expressed in the center-of-mass frame, which makes the calculation of the spectrum feasible. By analyzing the null geodesics, we identify the escape cones, i.e., the set of directions in the center-of-mass frame along which the massless particle must be emitted so that it escapes to infinity. We show that the escape cones span almost half of the entire angular range. We compute the conserved energy of the massless particle, which

is its energy as measured by an asymptotic observer if it escapes to infinity. We show that particles that escape along almost all the angles within the escape cones have divergent energies, while the particles that escape with finite energies are in minuscule minority. The conserved energy of the particles emitted in the opposite direction to that of the ultra-high-energy particles reaching infinity tends to negative infinity. This implies that the collisional Penrose process is at work and is responsible for the generation of ultra-high-energy particles in the overspinning Kerr geometry. These results do not depend on whether the center-of-mass frame moves radially outwards, radially inwards or does not admit any motion in the radial direction.

We show that all the ultra-high-energy particles have positive angular momenta and almost the same values of the impact parameter and thus the particles co-rotate with the singularity. A distant observer sees the ultra-high-energy particles originating from a bright spot which is located at the specific location on that side of the singularity which is rotating towards the observer. We computed the spectrum of the ultra-high-energy particles assuming that the cross section of the underlying particle physics process is constant at the large center-of-mass energies and distribution of the angular momenta of the colliding particles is uniform. We consider the case where the emission of the massless particles in the center-of-mass frame is isotropic as well the case where the emission is anisotropic with the anisotropy parametrized in a specific way. We find that there is an upper bound on the energy of the massless particle. The upper bound however can go to infinity in the near-extremal limit. The functional form of the energy distribution function is different above and below the upper bound. We show that the anisotropy of emission in the center-of-mass frame has its signature imprinted on the spectrum. Since the anisotropy is dictated by the differential cross section of the particle physics process, the observation of the spectrum can put constraints on and distinguish different particle physics models at high energies.

Thus, a near-extremal overspinning Kerr geometry will allow us to kill two birds with one stone. Firstly it would provide a mechanism to generate ultra-high-energy particles starting from the particles with moderate energies employing the collisional Penrose process with divergent efficiency and secondly the observation of the spectrum of high-energy particles would allow us to distinguish the different particle physics models. Hence, the existence of near-extremal overspinning Kerr geometry either as a permanent or a transient configuration would have a deep impact on the astrophysics as well as the fundamental particle physics.

If the backreaction is taken into account then the over-spinning Kerr geometry is driven towards the extremal Kerr black hole configuration. The calculation in this paper is meaningful only so long as the final spin parameter is larger than the extremal value. This puts an upper bound on

the energy of the massless particle. We show that the upper bound is still so high that it can be of great interest from astrophysical and particle physics point of view.

#### acknowledgement

T.H. and M.P. would like to thank T. Igata and K. Ogasawara for fruitful discussion. M.K. is partially supported by a grant for research abroad from JSPS. M.K. acknowledges financial support provided under the European Union’s H2020 ERC Consolidator Grant “Matter and strong-field gravity: New frontiers in Einstein’s theory” grant agreement no. MaGRaTh-646597, and under the H2020-MSCA-RISE-2015 Grant No. StronGrHEP-690904. M.P. was supported by the Research Center for Measurement in Advanced Science in Rikkyo University. This work was partially supported by JSPS KAKENHI Grant Number 26400282.

- 
- [1] J. Linsley, Phys. Rev. Lett. **10**, 146 (1963).
  - [2] L. Watson, D. Mortlock, A. Jaffe, MNRAS **418**, 206 (2011).
  - [3] A. Hillas, Annu. Rev. Astron. Astrophys **22** (1984).
  - [4] K. Kotera, A. Olinto, Annu. Rev. Astron. Astrophys **49** (2011).
  - [5] A. Letessier-Selvon, T. Stanev, Rev. Mod. Phys, **83**, 907 (2011).
  - [6] K. Greisen, Phys. Rev. Lett. **16**, 748 (1966).
  - [7] G. Zatsepin, V. Kuzmin, JETP Lett. **4**, 78 (1966).
  - [8] M. Aartsen et al. (IceCube Collaboration), Phys. Rev. Lett. **111**, 021103 (2013).
  - [9] M. Aartsen et al. (IceCube Collaboration), Phys. Rev. Lett. **113**, 101101 (2014).
  - [10] IceCube Collaboration, Nature, **484**, 351, (2012).
  - [11] R. Kerr, Phys. Rev. Lett. **11**, 237 (1963).
  - [12] R. Penrose, Nuovo Cimento, **1**, 252 (1969).
  - [13] R. Penrose, G. Flyod, Nature (London), Phy. Sci. **229**, 177 (1971).
  - [14] J. Bardeen, W. Press, S. Teukolsky, J. **178**, 347 (1972)
  - [15] R. Wald, Astrophys. J. **191**, 231 (1974).
  - [16] T. Piran, J. Shaham, J. Katz, Astrophys. J. **196**, L107 (1975).
  - [17] T. Piran, J. Shaham, Phys. Rev. D **16**, 1615 (1977).
  - [18] M. Banados, J. Silk, S.M. West, Phys. Rev. Lett. **103**, 111102 (2009).
  - [19] T. Harada, M. Kimura, Class. Quant. Grav. **31**, 243001 (2014).
  - [20] M. Cannoni, M. Gomez, M. Perez-Garcia, J. Vergados, Phys. Rev. D **85**, 115015 (2012).
  - [21] C. Arina, T. Bringmann, J. Silk, M. Vollmann, Phys. Rev. D **90**, 083506 (2014).

- [22] M. Bejger, T. Piran, M. Abramowicz, F. Hakanson, *Phys. Rev. Lett.* **109**, 121101 (2012).
- [23] T. Harada, H. Nemoto, U. Miyamoto, *Phys. Rev. D* **87**, 127502 (2013).
- [24] M. Banados, B. Hassanain, J. Silk, S.M. West, *Phys. Rev. D* **83**, 023004 (2011).
- [25] A. Williams, *Phys. Rev. D* **83**, 123004 (2011).
- [26] S. McWilliams, *Phys. Rev. Lett.* **110**, 011102 (2013).
- [27] J. Schnittman, *Phys. Rev. Lett.* **113**, 261102 (2014).
- [28] E. Berti, R. Britto, V. Cardoso, *Phys. Rev. Lett.* **114** 251103 (2015).
- [29] O. Zaslavskii, *JETP Lett.* **92**, 571 (2010).
- [30] O. Zaslavskii, *Phys. Rev. D* **86**, 124039 (2012).
- [31] H. Nemoto, U. Miyamoto, T. Harada, T. Kokubu, *Phys. Rev. D* **87**, 127502 (2013).
- [32] K. Nakao, M. Kimura, T. Harada, M. Patil, P. Joshi, *Phys. Rev. D* **90**, 124079 (2014).
- [33] T. Jacobson, T. Sotiriou, *Phys. Rev. Lett.* **103**, 209903 (2009).
- [34] E. Barausse, V. Cardoso, G. Khanna, *Phys. Rev. Lett.* **105**, 261102 (2010).
- [35] M. Colleoni, L. Barack, *Phys. Rev. D* **91**, 104024 (2015).
- [36] E. Gimon, P. Horava, *Phys. Lett. B* **672**, 299 (2009).
- [37] G. Horowitz, A. Sen, *Phys. Rev. D* **53**, 808 (1996).
- [38] G. Dotti, R. Gleiser, I. Ranea-Sandoval, *Class. Quant. Grav.* **29**, 095017 (2012).
- [39] V. Cardoso, P. Pani, M. Cadoni, M. Cavaglia, *Class. Quant. Grav.* **25**, 195010 (2008).
- [40] P. Pani, E. Barausse, E. Berti, V. Cardoso, *Phys. Rev. D* **82**, 044009 (2010).
- [41] M. Patil, P. Joshi, *Class. Quant. Grav.* **28**, 235012 (2011).
- [42] M. Patil, P. Joshi, *Phys. Rev. D* **84**, 104001 (2011).
- [43] M. Patil, P. Joshi, M. Kimura, K. Nakao, T. Harada, *EPL*, **110**, 30004 (2015).
- [44] M. Patil, P. Joshi, M. Kimura, K. Nakao, *Phys. Rev. D* **86**, 084023 (2012).
- [45] M. Patil, P. Joshi, arXiv:1106.5402 (2011).
- [46] O. Zaslavskii, *Phys. Rev. D* **88**, 044030 (2013).